SIAM J. APPL. MATH.
Vol. 80, No. 1, pp. 543–571

THE BASAL LAYER OF THE EPIDERMIS: A MATHEMATICAL MODEL FOR CELL PRODUCTION UNDER A SURFACE DENSITY CONSTRAINT*

ALBERTO GANDOLFI†, MIMMO IANNELLI‡, AND GABRIELA MARINOSCHI§

After submitting the manuscript, our dear friend Alberto Gandolfi died suddenly on a day in August and will not see this paper published. We will miss his sincere friendship and his valuable contribution to our collaboration.

Abstract. An age-structured model for the cell populations of the epidermis basal layer is proposed, with the aim of quantifying the cell production which makes possible epidermis renewal. The model, which extends our previous model [*J. Math. Biol.*, 73 (2016), pp. 1595–1626], describes the dynamics of proliferating cells, differentiated cells, and apoptotic cells under the physical constraint on the total surface cell density imposed by the cell occupancy of a basement membrane. To fulfill this constraint during any dynamics, the surface cell density is assumed to control cell migration toward the epidermis suprabasal region, as well as the balance between production of proliferating and of differentiated cells at cell division. The well-posedness of the model is fully studied, and the unique steady state is characterized. Numerical simulations are provided for realistic values of the parameters, giving some insight into the stability of the equilibrium and into the homeostatic properties of the model.

Key words. nonlinear PDE, population dynamics, age structure, numerical methods, epidermis, basal layer

AMS subject classifications. 35L03, 35L40, 65C20, 65M12, 65M25, 68U20, 92B05, 92C37, 92D25

DOI. 10.1137/19M1267052

1. Introduction.

The epidermis, which is the external part of the skin and so the ultimate protective barrier of the body, is a stratified epithelium that undergoes a continuous renewal process. The source of cells that sustains such a renewal is located in the basal layer, the innermost epidermis layer, where proliferation of cells occurs. Proliferating cells produce differentiated, nonproliferating cells (postmitotic keratinocytes) that detach from the underlying basement membrane and move outward forming the suprabasal layers (see Houben, De Paepe, and Rogiers [16]). Suprabasal cells undergo a progressive maturation, during which the keratin, a fibrous protein, accumulates in the cytoplasm. At the end of this process, the keratinocytes die, and the dead cells (called corneous cells or corneocytes) form the stratum corneum. The inner cells of the stratum corneum adhere to each other, but, when the corneocytes are pushed to the surface by newly formed cells, they lose their adhesion and eventually are shed from the epidermis surface [16].

*Received by the editors June 10, 2019; accepted for publication (in revised form) December 18, 2019; published electronically February 20, 2020.
https://doi.org/10.1137/19M1267052
Funding: This work was performed within the framework of the Italian-Romanian Project "Control and Stabilization Problems for Phase Field and Biological Systems," 2017–2019, funded by the CNR (Italy) and the Romanian Academy (Romania).
†The author is deceased. Former address: Istituto di Analisi dei Sistemi ed Informatica "A. Ruberti"-CNR, Rome, Italy (alberto.gandolfi@iasi.cnr.it).
‡Department of Mathematics, University of Trento, Trento, Italy (mimmo.iannelli@unitn.it).
§Gheorghe Mihoc-Caius Iacob Institute of Mathematical Statistics and Applied Mathematics, Romanian Academy, Bucharest, Romania (gabriela.marinoschi@acad.ro).

Until recently, the cell proliferation in the basal layer of epidermis was thought to follow the *stem cell–transit amplifying cell* scheme. In this scheme, a stem cell, which is endowed with an unlimited proliferative capability, produces by asymmetric division one stem cell and one progenitor cell that is able to undergo only a finite number of cell divisions (i.e., one transit amplifying cell). During the proliferation of transit amplifying cells, cell divisions are symmetric, producing two transit amplifying cells, and only at the last mitosis differentiated keratinocytes are originated (see Watt [34]). Such a hierarchy of cell populations has been mathematically analyzed at equilibrium in terms of cell age densities by Savill [33].

However, the existence of transiently proliferating cells has been challenged by Jones et al. [7, 22], who proposed that a single population of proliferating cells (called committed progenitors) exists and that these cells may undergo an unlimited number of divisions both symmetric and asymmetric, reproducing themselves or originating differentiated cells (*single-progenitor* scheme). This view has been partially reconciled with a stem cell–based model by Mascré et al. [28], who evidenced, in the mice epidermis, the existence of two kinetically different cell populations (stem cells and committed progenitor cells), supporting the hypothesis that both such populations have an unlimited mitotic capability (*stem/progenitor* scheme). In [28] it is also suggested that epidermis homeostasis is mainly due to proliferation of committed progenitors (in agreement with the Jones model), restricting the role of stem cells to the phase of tissue repair. These two populations could also be distinguished on the basis of molecular markers, in agreement with previous findings by Jensen and Watt [20].

More recently in Sada et al. [32], a markers technique allowed identifying two stem cell populations, coexisting in the basal layer with different proliferating rates, and supported the need of a model based on a *two-stem* scheme. However, the two populations are spatially segregated, but in the occurrence of epidermis repair, and both contribute to normal homeostasis, within distinct territories. Also, in Rompolas et al. [31], imaging techniques in live mice allowed following individual cells through their lifetime, following their movement through the suprabasal layer. In contrast with Sada's conclusions their findings support the existence of a single equipotent stem cell population in the basal layer, undergoing nonasymmetrical division and direct differentiation.

Although the unlimited mitotic capability of progenitor cells is rather controversial (see, for instance, Kaur and Potten [23]), the model we present in this paper is based on the *single-progenitor* scheme proposed by Jones et al. [7, 22]. Indeed, we disregard proliferation of stem cells, since their contribution to normal homeostasis is scarce, as commented on in Mascré et al. [28]. We mention that, however, the proliferative scheme suggested in [28] has been adopted in a recent mathematical ODE model of epidermis homeostasis by Zhang et al. [35], in connection with psoriasis pathology. Actually, our model can be somewhat reconciled with the existence of two proliferating populations found by Sada et al. [32] because the two populations are actually segregated and our model can be applied to the regions pertaining to the highly proliferating cells. Instead, since our model is based on asymmetric division, it does not follow the findings of Rompolas et al. [31].

Indeed, the model we present in detail in section 2 concerns only the basal layer and implements our previous models proposed to describe epidermis. In fact, in [10, 11] we proposed a model with age and space structure for the evolution of the suprabasal epidermis. In [10], after the formulation of the suprabasal model in its evolutive form, we focused on the existence and uniqueness of the stationary state,

proving it by a fixed point argument. In [11], we studied the existence of the time dependent solution. In the successive paper [12] we coupled a model of the cell proliferation in the basal layer with our previous model of the suprabasal evolution, obtaining a full model of the epidermis that we studied at the steady state. Such a steady state describes the spatial organization of the normal epidermis, or the new epidermal structure that may be reached after prolonged and time-invariant damaging.

In the present paper, we reconsider the age-structured model of the basal layer previously proposed in [12] and fully study the new formulation. The previous model guaranteed at the equilibrium state the fulfillment of the physical constraint on the surface cell density imposed by the cell occupancy of the basement membrane. The present model is intended to satisfy such constraint during any dynamics. Its formulation is described in section 2. In section 3, the well-posedness of the model and the fulfillment of the density constraint along any evolutive solution are proved. The existence of a unique nontrivial stationary solution is shown in section 4, where the stability of this equilibrium state is also briefly discussed. Numerical simulations are reported in section 5.

2. A model for cell production in the basal layer. The basal compartment of epidermis is arranged as a monolayer of parallelepipedal cells linked to the underlying basement membrane by integrin bonds. According to the *single-progenitor* scheme proposed in Clayton et al. [7], as mentioned above, committed progenitor cells (in the following, proliferating cells) divide both symmetrically producing two proliferating or two differentiated cells, and asymmetrically producing one proliferating cell and one differentiated cell. Basal mitoses can have different orientations, parallel to the basement plane or approximately orthogonal to that plane. In the orthogonal mitoses, one of the "daughter" cells lies on the basal layer, whereas the other cell is placed suprabasally on the top. Lerchler in [26, 29] proposed that the orthogonality of asymmetric mitoses is the main mechanism to transfer differentiated cells to the suprabasal region. However, the relative extent and the role of orthogonal mitoses in the mature nonembryonic epidermis is still debated. Clayton et al. [7] found that the vast majority of basal mitoses in the mouse tail epidermis, even in the case of asymmetric divisions, produce two basal-layer cells (only 3% of divisions were perpendicular). More recently, Ipponjima, Hibi, and Nemoto [19], by measuring the angle between the line through the nuclei at mitosis and the basement plane, found that in the dorsal and ear epidermis of mice more than 90% of divisions were at 0°–20°, while in the hind paw and interscale tail epidermis 30% of divisions were oblique (20°–70°) and 70% parallel. Orthogonal mitoses (70°–90°) were rarely observed in any epidermis region.

On the basis of these findings, and also for simplicity, we disregard the possible contribution of orthogonal mitoses to the migration of keratinocytes into the suprabasal region, and assume

(i) all the cell divisions occur in the basement plane;
(ii) differentiated cells detach and migrate into the suprabasal region after spending some time in the basal layer;
(iii) in some pathological cases proliferating cells can leave the basal layer and divide suprabasally (see [4, 24]);
(iv) in the presence of injuring factors that induce cell death, also apoptotic cells can enter the suprabasal region.

Although we did not find in the literature a clear experimental evidence of this last phenomenon (indeed its possibility was suggested in Bernerd, Sarasin, and

Magnaldo [2]) we include this assumption to have a model ready for possible exploration in the case of sound evidence of the transfer of apoptotic cells to the suprabasal zone.

As already assumed for our previous model in [12], also in the present model, the surface densities of the different cell subpopulations are considered spatially uniform and we disregard any possible net cell motion on the basement membrane. Moreover, we disregard any mechanical interaction between cells and signaling cues.

Let us denote by Ψ the surface fraction of basement membrane occupied by cells. Since some interstitial space is necessary to the cell life, it must be $\Psi < 1$. An expression for Ψ could be obtained by introducing the surface occupied by single cells of the different populations involved. However, this information appears experimentally uncertain, and so we consider simply an average value σ_c for the surface occupied by a single cell irrespective of its type or age. Thus, we have

$$\Psi(t) = \sigma_c \; N(t),$$

where $N(t)$ denotes the total number of basal cells per unit surface at time t. The density $N(t)$ must then satisfy the following constraint:

$$0 \leq N(t) < N_{max} \; = \; \frac{1}{\sigma_c}. \tag{2.1}$$

Since cells in the basal layer of normal epidermis appear to be close-packed, it is likely that in normal epidermis N takes a value close to N_{max}.

The populations of proliferating cells, differentiated cells, and dead cells will be described by age densities of the number of cells per unit surface; thus we denote by $\nu_P(a,t) \geq 0$, $\nu_D(a,t) \geq 0$, $\nu_A(a,t) \geq 0$ the age density, at time t, of proliferating, differentiated, apoptotic cells, respectively. In Figure 1 cell dynamics is schematically represented showing the *cell division* process, together with *detachment* and *apoptosis*.

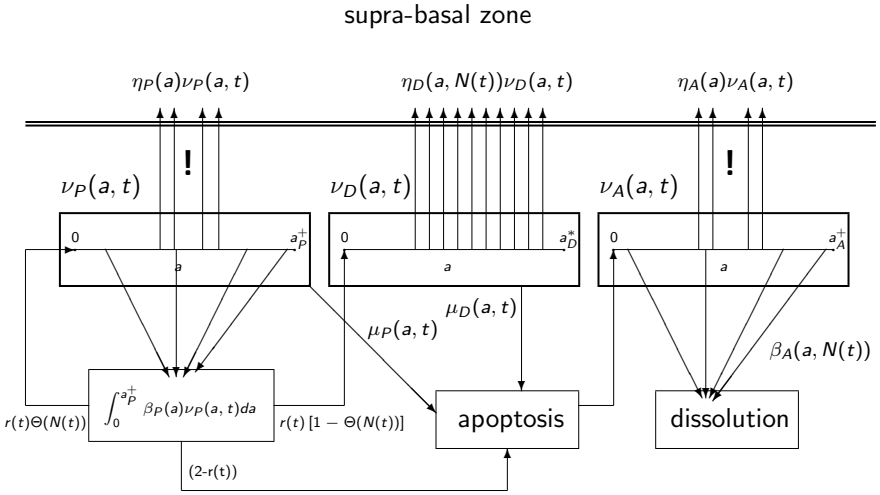

FIG. 1. *Schematic description of the model, showing asymmetric division of proliferating cell, production of differentiated cells and their migration into the suprabasal zone (over the double line), apoptosis and dissolution of apoptotic cells. See text for details about parameters. Migration of proliferating and apoptotic cells into the suprabasal layer is intended to possibly occur only exceptionally, for instance, in pathological situations (marked with the symbol* **!**).

Concerning *division* of proliferating cells, the process is governed by the following terms:

- $\beta_P(a)$ = per cell division rate of proliferating cells;
- $r(t)$ = mean number of viable daughter cells after a cell division;
- $\theta(N)$ = fraction of viable daughter cells that are still proliferating cells.

The rate $\beta_P(a) \geq 0$ is age dependent to account for the actual distribution of the cell cycle duration. The cell cycle time length is supposed to have an upper bound $a_P^+ < +\infty$, and then $\beta_P(a)$ is assumed to blow up at $a = a_P^+$ (see A3).

The term $r(t)$ accounts for possible abortive mitoses and $0 < r(t) \leq 2$. Under normal, unperturbed conditions $r = 2$; otherwise, in the presence of damaging factors, r will be less than 2.

Finally, the function $\theta(N) \in [0, 1]$ takes into account the co-presence of symmetric and asymmetric divisions. The production of differentiated cells is assumed to depend on the total population N. Cells may indeed sense cell crowding by responding to the mechanical stress due to cell-cell contact (see Chaplain, Graziano, and Preziosi [6] and references therein) and/or to the concentration of chemical factors that may accumulate in the cell microenvironment (see, e.g., d'Onofrio and Tomlinson [9] and Johnston et al. [21]). We assume that $\theta(N)$ satisfies

A1
$$\theta(N) \ \textit{ is a } \ C^1 \ \textit{ decreasing function on } \ [0, N_{max}] \ \textit{ such that}$$
$$\theta(0) = 1 \quad \textit{and} \quad 0 \leq \theta(N_{max}) < \tfrac{1}{2}.$$

By this assumption, as N approaches its physical limit N_{max}, the output of cell proliferation is forced to shift toward nonproliferating cells.

In summary, division of proliferating cells splits into the three parts

$$r(t)\theta(N(t)) \int_0^{a_P^+} \beta_P(a)\nu_P(a,t)da,$$
$$r(t)(1-\theta(N(t))) \int_0^{a_P^+} \beta_P(a)\nu_P(a,t)da,$$
$$(2-r(t)) \int_0^{a_P^+} \beta_P(a)\nu_P(a,t)da,$$

respectively feeding proliferating, differentiated, and apoptotic cells (see Figure 1).

As for *detachment*, we consider the nonnegative functions $\eta_P(a)$, $\eta_D(a, N)$, and $\eta_A(a)$ representing the per cell rate of detachment and migration into the suprabasal region of proliferating cells, differentiated cells, and apoptotic cells, respectively. Whereas the rates $\eta_P(a)$, $\eta_A(a)$ may be identically equal to zero (as in the case of healthy epidermis), the rate $\eta_D(a, N)$ must blow up at some age a_D^*, small with respect to the minimal age at which keratinocytes become corneous cells. In fact, the maturation of differentiated cells that leads to the generation of corneocytes occurs in the suprabasal region. Moreover, as a function of the total population N, $\eta_D(a, N)$ is supposed to blow up at N_{max} because we suppose that overcrowding of the basal layer forces the process of detachment of differentiated cells. In particular we assume

$$\eta_D(a, N) = \eta_D^0(a) + \eta_D^1(a)H(N), \tag{2.2}$$

where $\eta_D^0(a) \geq 0$ blows up at a_D^* and $\eta_D^1(a) \geq \bar{\eta}_D > 0$ is bounded (see A3). Dependence on the total number of cells is accounted through the function $H(N)$ satisfying the assumption

A2 $H(N)$ *is a* C^1 *increasing function on* $[0, N_{max})$ *such that*

$$H(0) = 0 \quad \textit{and} \quad \lim_{x \to N_{max}} H(x) = +\infty.$$

Finally, concerning *apoptosis*, apoptotic cells are produced both during the division process of proliferating cells and through the rates $\mu_P(a,t)$ and $\mu_D(a,t)$ that describe the action of possible external killing agents and the spontaneous cell death. Their population is taken into account as part of the total population because, though dead, these cells occupy some volume in the basal layer for some time before dissolution into the interstitial liquid. Moreover, it appears likely that the mechanical stress due to cell crowding can favor the degradation of dead cells into a liquid waste. Thus, we will assume that dissolution of apoptotic cells occurs at a rate $\beta_A(a, N(t))$ and is defined by

$$\beta_A(a,N) = \beta_A^0(a) + \beta_A^1(a)H(N), \tag{2.3}$$

where $\beta_A^0(a) \geq 0$ blows up at a_A^+, $\beta_A^1(a) \geq \bar{\beta}_A > 0$ is bounded (see A3), and the function $H(N)$ is the same function used in (2.2), satisfying assumption A2.

Note that the assumptions A1 and A2 guarantee that the physical constraint $N(t) < N_{max}$ will be satisfied not only at the stationary state but even for any solution of system (2.6)–(2.9) (see section 3).

After the above description of the processes, along the scheme shown in Figure 1, we can quantify the flow of differentiated cells into the suprabasal region by the flow age density $S_D(a,t)$ (note that $S_D(a,t)da$ gives the number of differentiated cells with age between a and $a + da$ that migrate, at time t, per unit time and per unit surface). In fact, the above flow age density is given by

$$S_D(a,t) = \eta_D(a, N(t))\nu_D(a,t), \tag{2.4}$$

while the possible flow densities $S_P(a,t)$ and $S_A(a,t)$ of proliferating and, respectively, of apoptotic cells are expressed by

$$S_P(a,t) = \eta_P(a)\nu_P(a,t), \quad S_A(a,t) = \eta_A(a)\nu_A(a,t). \tag{2.5}$$

Based on the previous description, our model is represented by the following system of equations, with their respective boundary condition at $a = 0$:

$$\begin{aligned} &\frac{\partial \nu_P}{\partial t} + \frac{\partial \nu_P}{\partial a} = -(\beta_P(a) + \eta_P(a) + \mu_P(a,t))\nu_P(a,t), \\ &\nu_P(0,t) = r(t)\theta(N(t)) \int_0^{a_P^+} \beta_P(a)\nu_P(a,t)da, \end{aligned} \tag{2.6}$$

$$\begin{aligned} &\frac{\partial \nu_D}{\partial t} + \frac{\partial \nu_D}{\partial a} = -(\eta_D(a, N(t)) + \mu_D(a,t))\nu_D(a,t), \\ &\nu_D(0,t) = r(t)(1 - \theta(N(t))) \int_0^{a_P^+} \beta_P(a)\nu_P(a,t)da, \end{aligned} \tag{2.7}$$

$$\begin{aligned} &\frac{\partial \nu_A}{\partial t} + \frac{\partial \nu_A}{\partial a} = -(\beta_A(a, N(t)) + \eta_A(a))\nu_A(a,t), \\ &\nu_A(0,t) = \int_0^{a_P^+} \big(\mu_P(a,t) + (2 - r(t))\beta_P(a)\big)\nu_P(a,t)da + \int_0^{a_D^*} \mu_D(a,t)\nu_D(a,t)da, \end{aligned} \tag{2.8}$$

where $N(t)$ is given by

$$N(t) = \int_0^{a_P^+} \nu_P(a,t)da + \int_0^{a_D^*} \nu_D(a,t)da + \int_0^{a_A^+} \nu_A(a,t)da \tag{2.9}$$

and must satisfy the constraint

$$0 \le N(t) < N_{max}.$$

These equations form an evolution system to be completed with initial conditions

$$\nu_P(a,0) = \nu_P^0(a) \ge 0, \quad \nu_D(a,0) = \nu_D^0(a) \ge 0, \quad \nu_A(a,0) = \nu_A^0(a) \ge 0 \tag{2.10}$$

with the constraint

$$\int_0^{a_P^+} \nu_P^0(a)da + \int_0^{a_D^*} \nu_D^0(a)da + \int_0^{a_A^+} \nu_A^0(a)da = N^0 < N_{max}\ . \tag{2.11}$$

We end this section by summarizing the mathematical assumptions that, together with A1 and A2, we will consider fulfilled throughout the paper:

A3
$$\begin{aligned}
&\beta_P \in L^1_{loc}([0,a_P^+)), \quad \beta_P(a) \ge 0 \ \text{ a.e.}, \quad \int_0^{a_P^+} \beta_P(a)da = +\infty,\\
&\beta_A^0 \in L^1_{loc}([0,a_A^+)), \quad \beta_A^0(a) \ge 0 \ \text{ a.e.}, \quad \int_0^{a_A^+} \beta_A^0(a)da = +\infty,\\
&\beta_A^1 \in L^\infty(0,a_A^+), \quad \beta_A^1(a) \ge \bar\beta_A > 0 \ \text{ a.e.},\\
&\eta_P \in L^\infty(0,a_P^+), \quad \eta_P(a) \ge 0 \ \text{ a.e.},\\
&\eta_D^0 \in L^1_{loc}([0,a_D^*)), \quad \eta_D^0(a) \ge 0 \ \text{ a.e.}, \quad \int_0^{a_D^*} \eta_D^0(a)da = +\infty,\\
&\eta_D^1 \in L^\infty(0,a_D^*), \quad \eta_D^1(a) \ge \bar\eta_D > 0 \ \text{ a.e.},\\
&\mu_P \in C([0,+\infty), L^\infty(0,a_P^+)), \quad \mu_P(a,t) \ge 0 \ \text{ a.e.},\\
&\mu_D \in C([0,+\infty), L^\infty(0,a_D^*)), \quad \mu_D(a,t) \ge 0 \ \text{ a.e.},\\
&r \in C([0,+\infty)), \quad 0 < r(t) \le 2.
\end{aligned}$$

3. Well-posedness of the model. The model presented in the previous section falls within the class of age-structured models and can be treated with classical methods to prove existence and uniqueness. Here we adopt the direct method based on the transformation into integral equations (see, for instance, [18]). The full proof of well-posedness will be split into three steps to help the presentation.

3.1. Transformation of the problem. As a first step, we will transform the problem considering the new variables $\tilde\nu_P(a,t), \tilde\nu_D(a,t), \tilde\nu_A(a,t)$ through the following definitions:

$$\tilde\nu_P(a,t) = \frac{\nu_P(a,t)}{M_P(a)E_P(a)}, \quad \tilde\nu_D(a,t) = \frac{\nu_D(a,t)}{E_D^0(a)}, \quad \tilde\nu_A(a,t) = \frac{\nu_A(a,t)}{M_A^0(a)E_A(a)}, \tag{3.1}$$

where

$$M_P(a) = e^{-\int_0^a \beta_P(\sigma)d\sigma}, \quad M_A^0(a) = e^{-\int_0^a \beta_A^0(\sigma)d\sigma},$$

$$E_P(a) = e^{-\int_0^a \eta_P(\sigma)d\sigma}, \quad E_D^0(a) = e^{-\int_0^a \eta_D^0(\sigma)d\sigma}, \quad E_A(a) = e^{-\int_0^a \eta_A(\sigma)d\sigma}.$$

In these new variables problem (2.6)–(2.9) becomes (dropping the tildes for notational simplicity)

$$\begin{aligned} &\frac{\partial \nu_P}{\partial t} + \frac{\partial \nu_P}{\partial a} + \mu_P(a,t)\nu_P(a,t) = 0, \\ &\nu_P(0,t) = r(t)\theta(N(t)) \int_0^{a_P^+} K_P(a)\nu_P(a,t)da, \end{aligned} \tag{3.2}$$

$$\begin{aligned} &\frac{\partial \nu_D}{\partial t} + \frac{\partial \nu_D}{\partial a} + \big(\eta_D^1(a)H(N(t)) + \mu_D(a,t)\big)\nu_D(a,t) = 0, \\ &\nu_D(0,t) = r(t)(1-\theta(N(t))) \int_0^{a_P^+} K_P(a)\nu_P(a,t)da, \end{aligned} \tag{3.3}$$

$$\begin{aligned} &\frac{\partial \nu_A}{\partial t} + \frac{\partial \nu_A}{\partial a} + \beta_A^1(a)H(N(t))\nu_A(a,t) = 0, \\ &\nu_A(0,t) = \int_0^{a_P^+} \mu_P(a,t)k_P(a)\nu_P(a,t)da + \int_0^{a_D^*} \mu_D(a,t)k_D(a)\nu_D(a,t)da \\ &\qquad + (2-r(t)) \int_0^{a_P^+} K_P(a)\nu_P(a,t)da, \end{aligned} \tag{3.4}$$

$$N(t) = \int_0^{a_P^+} k_P(a)\nu_P(a,t)da + \int_0^{a_D^*} k_D(a)\nu_D(a,t)da + \int_0^{a_A^+} k_A(a)\nu_A(a,t)da, \tag{3.5}$$

where

$$\begin{aligned} &K_P(a) = \beta_P(a)M_P(a)E_P(a), \quad k_P(a) = M_P(a)E_P(a), \\ &k_D(a) = E_D^0(a), \quad k_A(a) = M_A^0(a)E_A(a). \end{aligned} \tag{3.6}$$

Of course, problem (3.2)–(3.5) is endowed with initial conditions $(\nu_P^0, \nu_D^0, \nu_A^0)$ coming from (2.10) through the normalization (3.1) and satisfying the constraint

$$\int_0^{a_P^+} k_P(a)\nu_P^0(a)da + \int_0^{a_D^*} k_D(a)\nu_D^0(a)da + \int_0^{a_A^+} k_A(a)\nu_A^0(a)da = N^0 < N_{max}. \tag{3.7}$$

As (3.2)–(3.7) is an evolution system, we may represent the three-components solution by the vector notation

$$\vec{\nu}(a,t;\vec{\nu}^{\,0}(\cdot)) \equiv (\nu_P(a,t),\ \nu_D(a,t),\ \nu_A(a,t))$$

showing the initial datum

$$\vec{\nu}^{\,0}(a) = (\nu_P^0(a), \nu_P^0(a), \nu_P^0(a)) \ .$$

With this notation we may notice the semigroup property of the system

$$\vec{\nu}(a,t+s;\vec{\nu}^{\,0}(\cdot)) = \vec{\nu}(a,t;\vec{\nu}(\cdot,s;\vec{\nu}^{\,0}(\cdot))) \ . \tag{3.8}$$

Following the approach in [18], the system can be represented in integral form as

$$\nu_P(a,t) = \begin{cases} B_P(t-a)e^{-\int_0^a \mu_P(a-\sigma,\ t-\sigma)d\sigma} & \text{if } \ a \le t, \\ \nu_P^0(a-t)e^{-\int_0^t \mu_P(a-\sigma,\ t-\sigma)d\sigma} & \text{if } \ t < a, \end{cases}$$

$$\nu_D(a,t) = \begin{cases} B_D(t-a)e^{-\int_0^a \left[H(N(t-\sigma))\eta_D^1(a-\sigma)+\mu_D(a-\sigma,\ t-\sigma)\right]d\sigma} & \text{if } \ a \le t, \\ \nu_D^0(a-t)e^{-\int_0^t \left[H(N(t-\sigma))\eta_D^1(a-\sigma)+\mu_D(a-\sigma,\ t-\sigma)\right]d\sigma} & \text{if } \ t < a, \end{cases} \tag{3.9}$$

$$\nu_A(a,t) = \begin{cases} B_A(t-a)e^{-\int_0^a H(N(t-\sigma))\beta_A^1(a-\sigma)d\sigma} & \text{if } \ a \le t, \\ \nu_A^0(a-t)e^{-\int_0^t H(N(t-\sigma))\beta_A^1(a-\sigma)d\sigma} & \text{if } \ t < a, \end{cases}$$

where $(B_P(t), B_D(t), B_A(t), N(t))$ solves the following system of integral equations:

$$\begin{aligned} B_P(t) = r(t)\theta(N(t)) \Bigg[& \int_0^t K_P(a)e^{-\int_0^a \mu_P(a-\sigma,\ t-\sigma)d\sigma} B_P(t-a)da \\ & + \int_t^\infty K_P(a)e^{-\int_0^t \mu_P(a-\sigma,\ t-\sigma)d\sigma}\nu_P^0(a-t)da \Bigg], \end{aligned} \tag{3.10}$$

$$\begin{aligned} B_D(t) = r(t)(1-\theta(N(t))) \Bigg[& \int_0^t K_P(a)e^{-\int_0^a \mu_P(a-\sigma,\ t-\sigma)d\sigma} B_P(t-a)da \\ & + \int_t^\infty K_P(a)e^{-\int_0^t \mu_P(a-\sigma,\ t-\sigma)d\sigma}\nu_P^0(a-t)da \Bigg], \end{aligned} \tag{3.11}$$

$$\begin{aligned} B_A(t) = & \int_0^t \mu_P(a,t)k_P(a)e^{-\int_0^a \mu_P(a-\sigma,\ t-\sigma)d\sigma} B_P(t-a)da \\ & + (2-r(t)) \int_0^t K_P(a)e^{-\int_0^a \mu_P(a-\sigma,\ t-\sigma)d\sigma} B_P(t-a)da \\ & + \int_0^t \mu_D(a,t)k_D(a)e^{-\int_0^a \left[H(N(t-\sigma))\eta_D^1(a-\sigma)+\mu_D(a-\sigma,\ t-\sigma)\right]d\sigma} B_D(t-a)da \\ & + \int_t^\infty \mu_P(a,t)k_P(a)e^{-\int_0^t \mu_P(a-\sigma,\ t-\sigma)d\sigma}\nu_P^0(a-t)da \\ & + (2-r(t)) \int_t^\infty K_P(a)e^{-\int_0^t \mu_P(a-\sigma,\ t-\sigma)d\sigma}\nu_P^0(a-t)da \\ & + \int_t^\infty \mu_D(a,t)k_D(a)e^{-\int_0^t \left[H(N(t-\sigma))\eta_D^1(a-\sigma)+\mu_D(a-\sigma,\ t-\sigma)\right]d\sigma}\nu_D^0(a-t)da, \end{aligned} \tag{3.12}$$

$$\begin{aligned} N(t) = & \int_0^t k_P(a)e^{-\int_0^a \mu_P(a-\sigma,\ t-\sigma)d\sigma} B_P(t-a)da \\ & + \int_0^t k_D(a)e^{-\int_0^a \left[H(N(t-\sigma))\eta_D^1(a-\sigma)+\mu_D(a-\sigma,\ t-\sigma)\right]d\sigma} B_D(t-a)da \\ & + \int_0^t k_A(a)e^{-\int_0^a H(N(t-\sigma))\beta_A^1(a-\sigma)d\sigma} B_A(t-a)da \\ & + \int_t^\infty k_P(a)e^{-\int_0^t \mu_P(a-\sigma,\ t-\sigma)d\sigma}\nu_P^0(a-t)da \end{aligned} \tag{3.13}$$

$$+\int_t^\infty k_D(a)e^{-\int_0^t\left[H(N(t-\sigma))\eta_D^1(a-\sigma)+\mu_D(a-\sigma,\ t-\sigma)\right]d\sigma}\nu_D^0(a-t)da$$
$$+\int_t^\infty k_A(a)e^{-\int_0^t H(N(t-\sigma))\beta_A^1(a-\sigma)d\sigma}\nu_A^0(a-t)da,$$

$$0\le N(t)<N_{max}. \tag{3.14}$$

where all the functions, initially defined in $[0,a_P^+]$, or $[0,a_D^*]$, or $[0,a_A^+]$, are extended as 0 outside their interval of definition.

Indeed, based on the above formulation of the problem, system (3.10)–(3.13) with nonnegative initial data ν_P^0, ν_D^0, ν_A^0 can be solved producing a set of nonnegative continuous functions B_P, B_D, B_A, N that, plugged into (3.9), provide a (unique) solution $(\nu_P(a,t),\nu_D(a,t),\nu_A(a,t))$ to (3.2)–(3.5). Actually, the solution obtained with this procedure may not be regular enough to fulfill (3.2)–(3.5) in a strict sense but, as is clear from the representation (3.9), the solution is differentiable along the characteristic lines $a-t=\text{const}$ (see [18]).

Though the proof of existence of a solution to (3.10)–(3.13) follows a standard argument, the problem presents some unusual features that to our knowledge have not been treated before, so that we cannot refer to known results and need to provide a detailed proof. In fact, the usual assumptions on the parameters of the equations imply that the kernel K_P defined in (3.6) is bounded on $[0,+\infty)$, while in our case it is integrable, but not necessarily bounded. Moreover, while usually such population problems have no constraint, in our case the problem is defined for $N\in[0,N_{max})$ (as the function $H(N)$ is) and consequently we look for a solution satisfying the constraint (3.7). In the following, we first consider a modified unconstrained case and then solve the full problem.

3.2. The unconstrained case. As a first step to the proof, we first consider the case without the constraint (3.7) supposing that the function $H(N)$ is defined on the whole interval $[0,+\infty)$ and is Lipschitz continuous:

$$\left|H(N)-H(\bar N)\right|\le L_H\left|N-\bar N\right|. \tag{3.15}$$

In fact we have the following.

THEOREM 3.1. *Suppose that the function $H:[0,+\infty)\to[0,+\infty)$ satisfies* (3.15). *Consider nonnegative initial data satisfying*

$$\nu_P^0\in C([0,a_P^+]),\quad \nu_D^0\in C([0,a_D^*]),\quad \nu_A^0\in C([0,a_A^+]). \tag{3.16}$$

Then problem (3.10)–(3.13) *has a unique nonnegative solution, continuous on* $\mathbf{R}_+$.

Proof. We start the proof considering (3.10) supposing $N\in C(\mathbf{R}_+,\mathbf{R}_+)$ is given and fixed. The solution of this equation can be obtained as a fixed point of the mapping $\mathcal{T}:C(\mathbf{R}_+,\mathbf{R}_+)\to C(\mathbf{R}_+,\mathbf{R}_+)$ defined as

$$\mathcal{T}(u)(t)=r(t)\theta(N(t))\left[\int_0^t K_P(a)e^{-\int_0^a\mu_P(a-\sigma,\ t-\sigma)d\sigma}u(t-a)da\right.$$
$$\left.+\int_t^\infty K_P(a)e^{-\int_0^t\mu_P(a-\sigma,\ t-\sigma)d\sigma}\nu_P^0(a-t)da\right].$$

In fact we have the estimate

$$e^{-\alpha t}\left|\mathcal{T}(u)(t)-\mathcal{T}(v)(t)\right|\le 2\int_0^{a_P^+}e^{-\alpha a}K_P(a)da\ \sup_{s\ge0}\{e^{-\alpha s}\left|u(s)-v(s)\right|\}$$

and, taking α large enough, say, $\alpha > \alpha^+$, so that

$$K_\alpha = \int_0^{a_P^+} e^{-\alpha a} K_P(a)da < \frac{1}{4}\ ,$$

we have that $\mathcal{T}$ is a contraction in the space

$$E \equiv \left\{ f \in C(\mathbf{R}_+, \mathbf{R}) \mid e^{-\alpha t} f(t) \quad \text{is bounded} \right\}$$

endowed with the norm

$$\|f\|_\alpha = \sup_{s\geq 0}\{e^{-\alpha s}\,|f(s)|\}.$$

In order to show the dependence on N, we will denote this solution $B_P(t;N)$. From the equation we can also draw the estimate[1]

$$\begin{aligned} e^{-\alpha t} B_P(t;N) &\leq 2\int_0^t e^{-\alpha a} K_P(a) e^{-\alpha(t-a)} B_P(t-a;N)da + \int_t^\infty K_P(a)da \left\|\nu_P^0\right\|_\infty \\ &\leq 2K_\alpha \left\|B_P(\cdot\,;N)\right\|_\alpha + \left\|\nu_P^0\right\|_\infty \end{aligned}$$

that, for $\alpha > \alpha^+$, implies

$$B_P(t;N) \leq \frac{2e^{\alpha t}}{1-2K_\alpha} \left\|\nu_P^0\right\|_\infty \leq 4e^{\alpha t} \left\|\nu_P^0(\cdot)\right\|_\infty . \tag{3.17}$$

Moreover we have

$$\begin{aligned} \left|B_P(t;N) - B_P(t;\bar N)\right| &\leq Ce^{\alpha t}\left|N(t) - \bar N(t)\right| \\ &\quad + 2\int_0^t K_P(a)\left|B_P(t-a;N) - B_P(t-a;\bar N)\right| da, \end{aligned}$$

where (for $\alpha > \alpha^+$) the constant C depends only on $\left\|\nu_P^0\right\|_\infty$ and on the Lipschitz constant of the function $\Theta(N)$. Then

$$\begin{aligned} &\int_0^t e^{-\alpha s}\left|B_P(s;N) - B_P(s;\bar N)\right| ds \\ &\quad \leq C\int_0^t \left|N(s) - \bar N(s)\right| ds \\ &\qquad + 2\int_0^t \int_0^s e^{-\alpha a} K_P(a) e^{-\alpha(s-a)} \left|B_P(s-a;N) - B_P(s-a;\bar N)\right| da\ ds \\ &\quad = C\int_0^t \left|N(s) - \bar N(s)\right| ds \\ &\qquad + 2\int_0^t e^{-\alpha a} K_P(a) \int_a^t e^{-\alpha(s-a)} \left|B_P(s-a;N) - B_P(s-a;\bar N)\right| ds\ da \\ &\quad \leq C\int_0^t \left|N(s) - \bar N(s)\right| ds + 2K_\alpha \int_0^t e^{-\alpha s}\left|B_P(s;N) - B_P(s;\bar N)\right| ds, \end{aligned}$$

and finally

$$\int_0^t e^{-\alpha s}\left|B_P(s;N) - B_P(s;\bar N)\right| ds \leq 2C\int_0^t \left|N(s) - \bar N(s)\right| ds. \tag{3.18}$$

[1]For any function f defined in any interval (a,b), we will denote its $L^\infty(a,b)$ norm by $\|f\|_\infty$.

Once we have $B_P(t;N)$ (as a function of N), we plug it into (3.11) and (3.12), obtaining $B_D(t;N)$ and $B_A(t;N)$ as functions of N, to be used later in (3.13). Using (3.17) and (3.18) we derive also the estimates

$$B_D(t;N) + B_A(t;N) \le Me^{\alpha t} \tag{3.19}$$

and

$$\int_0^t e^{-\alpha s}\Big(\big|B_D(s;N)-B_D(s;\bar N)\big|+\big|B_D(s;N)-B_D(s;\bar N)\big|\Big)ds \le M\int_0^t \big|N(s)-\bar N(s)\big|\,ds,$$

where, for $\alpha > \alpha^+$, M is a constant depending only on the parameters of the problem.

As a final step, we consider (3.13) and insert $B_P(s;N)$, $B_D(s;N)$, $B_A(s;N)$, obtaining a single equation in the variable $N(t)$. The solution will be found as a fixed point of the mapping $\mathcal{M} : C(\mathbf{R}_+,\mathbf{R}_+) \to C(\mathbf{R}_+,\mathbf{R}_+)$ defined as

$$\begin{aligned}
\mathcal{M}(u)(t) = &\int_0^t k_P(a)e^{-\int_0^a \mu_P(a-\sigma,\ t-\sigma)d\sigma}B_P(t-a;u)da\\
&+\int_0^t k_D(a)e^{-\int_0^a \left[H(u(t-\sigma))\eta_D^1(a-\sigma)+\mu_D(a-\sigma,\ t-\sigma)\right]d\sigma}B_D(t-a;u)da\\
&+\int_0^t k_A(a)e^{-\int_0^a H(u(t-\sigma))\beta_A^1(a-\sigma)d\sigma}B_A(t-a;u)da\\
&+\int_t^\infty k_P(a)e^{-\int_0^t \mu_P(a-\sigma,\ t-\sigma)d\sigma}\nu_P^0(a-t)da\\
&+\int_t^\infty k_D(a)e^{-\int_0^t H(u(t-\sigma))\eta_D^1(a-\sigma)d\sigma}\nu_D^0(a-t)da\\
&+\int_t^\infty k_A(a)e^{-\int_0^t H(u(t-\sigma))\beta_A^1(a-\sigma)d\sigma}\nu_A^0(a-t)da.
\end{aligned}$$

Indeed, using the estimate stated above we get

$$|\mathcal{M}(u)(t) - \mathcal{M}(\bar u)(t)| \le L\ e^{\alpha t}\int_0^t |u(s)-\bar u(s)|\,ds, \tag{3.20}$$

where, for $\alpha \ge \alpha^+$, L depends only on the parameters of the problem. In particular, to prove this inequality we need to use repeatedly estimates such as, for instance,

$$\begin{aligned}
&\int_0^t k_D(a)\left|e^{-\int_0^a H(u(t-\sigma))\eta_D^1(a-\sigma)d\sigma} - e^{-\int_0^a H(\bar u(t-\sigma))\eta_D^1(a-\sigma)d\sigma}\right| B_D(t-a;u)da\\
&\quad+\int_t^\infty k_D(a)\left|e^{-\int_0^t H(u(t-\sigma))\eta_D^1(a-\sigma)d\sigma} - e^{-\int_0^t H(\bar u(t-\sigma))\eta_D^1(a-\sigma)d\sigma}\right| \nu_D^0(a-t)da\\
&\quad\le Ce^{\alpha t}\left(\int_0^t k_D(a)\int_0^a |u(t-\sigma)-\bar u(t-\sigma)|\,d\sigma da + \int_t^\infty k_D(a)\int_0^t |u(t-\sigma)-\bar u(t-\sigma)|\,d\sigma da\right)\\
&\quad= Ce^{\alpha t}\left(\int_0^t\int_\sigma^t k_D(a)\,|u(t-\sigma)-\bar u(t-\sigma)|\,da d\sigma + \int_0^t\int_t^\infty k_D(a)\,|u(t-\sigma)-\bar u(t-\sigma)|\,da d\sigma\right)\\
&\quad= C\,\|k_D\|_1\,e^{\alpha t}\int_0^t |u(\sigma)-\bar u(\sigma)|\,d\sigma,
\end{aligned}$$

where C is a constant depending only on the parameters of the problem.

Inequality (3.20) allows us to prove that $\mathcal{M}$ is a contraction in the space $C([0,T])$ (for any $T>0$) endowed with the norm

$$\|f\|_\delta = \max_{s\in[0,T]} \left\{e^{-\delta s}|f(s)|\right\},$$

where δ is sufficiently large. In fact from (3.20) we have

$$\|\mathcal{M}(u)-\mathcal{M}(\bar u)\|_\delta \le \frac{L\ e^{\alpha T}}{\delta}\,\|u-\bar u\|_\delta\,.$$

Thus, for δ sufficiently large $\mathcal{M}$ has a unique fixed point solution in $C([0,T])$, i.e., problem (3.10)–(3.13) has a unique solution in this space. Since T is arbitrary, the thesis of the theorem is proved. ∎

As a direct consequence of Theorem 3.1, via the representation (3.9), we have a solution of (3.2)–(3.5) in the sense stated in the following.

COROLLARY 3.2. *Under the assumptions of Theorem* 3.1*, if the initial conditions satisfy the compatibility constraints*

$$\begin{aligned}
&\nu_P^0(0) = r(0)\theta(N^0)\int_0^{a_P^+} K_P(a)\nu_P^0(a)da, \quad \nu_D^0(0) = \frac{1-\theta(N^0)}{\theta(N^0)}\nu_P^0(0),\\
&\nu_A^0(0) = \int_0^{a_P^+}\mu_P(a,0)k_P(a)\nu_P^0(a)da + \int_0^{a_D^*}\mu_D(a,0)k_D(a)\nu_D^0(a)da\\
&\qquad + (2-r(0))\int_0^{a_P^+} K_P(a)\nu_P^0(a)da,
\end{aligned} \tag{3.21}$$

problem (3.2)–(3.5) *has a unique solution* $\vec\nu(a,t;\vec\nu\ ^0(\cdot)) \equiv (\nu_P(a,t),\ \nu_D(a,t),\ \nu_A(a,t))$ *where the components* $\nu_P(a,t),\ \nu_D(a,t),\ \nu_A(a,t)$ *are nonnegative and continuous and solve the problem in the sense that the directional derivatives* $(\partial/\partial t + \partial/\partial a)$ *exist and satisfy* (3.2)–(3.5).

Note that, due to (3.17) and (3.19), we have

$$\nu_P(0,t)+\nu_D(0,t)+\nu_A(0,t) \le Ce^{\alpha t}, \tag{3.22}$$

where the constant C depends on the parameters of the problem and on the initial data.

Finally, we remark that the compatibility conditions (3.21) guarantee continuity of the solution across the characteristic line $t-a=0$. If (3.21) are not satisfied, the solution is, however, continuous for $t\neq a$.

3.3. Well-posedness in the full case. The previous theorem is a first step to the treatment of the problem under assumption A2. Namely we have

THEOREM 3.3. *Suppose that the function* $H:[0,N_{max})\to[0,+\infty)$ *satisfies* A2 *and that the nonnegative initial data* (3.16) *fulfill* (3.7) *and* (3.21). *Then problem* (3.2)–(3.5) *has a unique solution* $\vec\nu(a,t;\vec\nu\ ^0(\cdot)) \equiv (\nu_P(a,t),\ \nu_D(a,t),\ \nu_A(a,t))$*, where the components* $\nu_P(a,t),\ \nu_D(a,t),\ \nu_A(a,t)$ *are nonnegative and continuous and satisfy the problem in the sense of the directional derivative. Moreover the constraint*

$$N(t) = \int_0^{a_P^+} k_P(a)\nu_P(a,t)da + \int_0^{a_D^*} k_D(a)\nu_D(a,t)da + \int_0^{a_A^+} k_A(a)\nu_A(a,t)da < N_{max} \tag{3.23}$$

is satisfied.

Proof. Let us first modify the function $H(N)$ in order to be able to apply the previous theorem. Namely, for any $\lambda \in (N^0, N_{max})$ (see (3.7)) we take a Lipschitz function $H_\lambda : [0, +\infty) \to [0, +\infty)$ such that

$$H_\lambda(N) = H(N) \quad \text{for} \quad N \in [0, \lambda]$$

and consider problem (3.2)–(3.5) with H_λ instead of H. By Corollary 3.2, for any λ, we have a (unique) solution that we denote $\nu_P^\lambda(a,t)$, $\nu_D^\lambda(a,t)$, $\nu_A^\lambda(a,t)$ together with the total population

$$N^\lambda(t) = \int_0^{a_P^+} k_P(a)\nu_P^\lambda(a,t)da + \int_0^{a_D^*} k_D(a)\nu_D^\lambda(a,t)da + \int_0^{a_A^+} k_A(a)\nu_A^\lambda(a,t)da \ .$$

Then we define

$$t_\lambda = \sup_{t\geq 0} \left\{ t \ \middle| \ N^\lambda(s) \leq \lambda \quad \text{for} \quad s \in [0,t] \right\}$$

so that, putting

$$\nu_P(a,t) = \nu_P^\lambda(a,t), \quad \nu_D(a,t) = \nu_D^\lambda(a,t), \quad \nu_A(a,t) = \nu_A^\lambda(a,t),$$

we get a (unique) solution to the original problem in the interval $[0, t_\lambda]$, satisfying the constraint (3.23).

Of course, if we can find a value for λ such that $t_\lambda = +\infty$, then the solution to the λ-problem is the sought solution to the original problem. Thus we focus on the case $t_\lambda < +\infty$ for all λ. In this case we note that if $\lambda_1 < \lambda_2$, since $H^{\lambda_1}(N) = H^{\lambda_2}(N)$ for $N \leq \lambda_1$, the solution to the λ_1-problem coincides with the solution to the λ_2-problem for $t \in [0, t_{\lambda_1}]$. Consequently $t_{\lambda_1} < t_{\lambda_2}$ and we can define

$$T = \lim_{\lambda \to N_{max}} t_\lambda$$

to build a unique solution to the original problem in the interval $[0, T)$, satisfying (3.23) for $t \in [0, T)$.

To conclude the proof of the theorem we are left with showing that $T = +\infty$. However, we first focus on the first equation (2.6) that does not depend on the function $H(\cdot)$ and note that, by the proof of the previous theorem, the estimate (3.22) holds also for the component ν_P of the present solution on the interval $[0, T)$. Moreover, we have a bound also for $N_P(t) = \int_0^{a_P^+} k_P(a)\nu_P(a,t)da$. In fact we consider N_P^* such that

$$N_P(0) < N_P^* < N_{max}, \quad \theta(N_P^*) < \frac{1}{2}, \tag{3.24}$$

and we prove that

$$N_P(t) \leq N_P^* \quad \text{for all} \ \ t \in [0, T). \tag{3.25}$$

Indeed if (3.25) was not true, we could find $t^* < T$ and $\varepsilon < a_P^+$, such that

$$N_P(t^*) = N_P^* \quad \text{and} \quad N_P^* < N_P(t) \leq N(t) \quad \text{for} \quad t^* < t \leq t^* + \varepsilon < T \ . \tag{3.26}$$

Now, from (3.6) and (3.2), the directional derivative of $k_P(a)\nu_P(a,t)$ reads

$$\begin{aligned} \left(\frac{\partial}{\partial t} + \frac{\partial}{\partial a}\right) k_P(a)\nu_P(a,t) &= -\left(\beta_P(a) + \eta_P(a) + \mu_P(a,t)\right) k_P(a)\nu_P(a,t) \\ &\leq -K_P(a)\nu_P(a,t) \end{aligned}$$

and, integrating along characteristic lines, we have

$$k_P(a)\nu_P(a,t) \le \begin{cases} \nu_P(0,t-a) - \displaystyle\int_0^a K_P(a-\sigma)\nu_P(a-\sigma,t-\sigma)d\sigma, & a < t-t^*, \\ k_P(a-t+t^*)\nu_P(a-t+t^*,t^*) & \\ \quad - \displaystyle\int_0^{t-t^*} K_P(a-\sigma)\nu_P(a-\sigma,t-\sigma)d\sigma, & a \ge t-t^*. \end{cases} \tag{3.27}$$

Consequently, we can estimate $N_P(t)$ as

$$\begin{aligned} N_P(t) \le{}& \int_0^{t-t^*} r(t-a)\theta(N(t-a))\int_0^{a_P^+} K_P(\sigma)\nu_P(\sigma,t-a)d\sigma da \\ &+ \int_{t-t^*}^{a_P^+} k_P(a-t+t^*)\nu_P(a-t+t^*,t^*)da - \int_0^{t-t^*}\int_0^a K_P(a-\sigma)\nu_P(a-\sigma,t-\sigma)d\sigma da \\ &- \int_{t-t^*}^{a_P^+}\int_0^{t-t^*} K_P(a-\sigma)\nu_P(a-\sigma,t-\sigma)d\sigma da. \end{aligned}$$

Now, by (3.26) in the first integral we have $N(t-a) \ge N_P(t-a) \ge N_P^*$, because $t^* \le t-a \le t^*+\varepsilon$; thus, with some change of variables and exchanging the order of some integrals, for $t^* \le t \le t^*+\varepsilon$, we have (see (3.24))

$$\begin{aligned} N_P(t) \le{}& 2\theta(N_P^*)\int_0^{t-t^*}\int_0^{a_P^+} K_P(\sigma)\nu_P(\sigma,t-a)d\sigma da + \int_0^{a_P^+-t+t^*} k_P(a)\nu_P(a,t^*)da \\ &-\int_0^{t-t^*}\int_\sigma^{t-t^*} K_P(a-\sigma)\nu_P(a-\sigma,t-\sigma)da d\sigma \\ &-\int_0^{t-t^*}\int_{t-t^*}^{a_P^+} K_P(a-\sigma)\nu_P(a-\sigma,t-\sigma)da d\sigma \\ \le{}& \int_0^{t-t^*}\int_\sigma^{a_P^+-\sigma} K_P(a-\sigma)\nu_P(a-\sigma,t-\sigma)da d\sigma + \int_0^{a_P^+-t+t^*} k_P(a)\nu_P(a,t^*)da \\ &- \int_0^{t-t^*}\int_\sigma^{a_P^+} K_P(a-\sigma)\nu_P(a-\sigma,t-\sigma)da d\sigma \\ ={}& N_P^* + \int_0^{t-t^*}\int_{a_P^+}^{a_P^+-\sigma} K_P(a-\sigma)\nu_P(a-\sigma,t-\sigma)da d\sigma - \int_{a_P^+-t+t^*}^{a_P^+} k_P(a)\nu_P(a,t^*) \le N_P^*. \end{aligned} \tag{3.28}$$

Indeed, the last inequality holds because from (3.27) we have

$$k_P(a_P^+-t+t^*)\nu_P(a_P^+-t+t^*,t^*) \ge \int_0^{t-t^*} K_P(a_P^+-\sigma)\nu_P(a_P^+-\sigma,t-\sigma)d\sigma$$

for $t \in [t^*, t^*+\varepsilon]$. Then, setting $s = a_P^+ - t + t^*$ in this inequality we have

$$\begin{aligned} k_P(s)\nu_P(s,t^*) &\ge \int_0^{a_P^+-s} K_P(a_P^+-\sigma)\nu_P(a_P^+-\sigma,a_P^++t^*-s-\sigma)d\sigma \\ &= \int_0^{a_P^+-s} K_P(s+\sigma)\nu_P(s+\sigma,t^*+\sigma)d\sigma \end{aligned}$$

for $s \in [a_P^+ - \varepsilon, a_P^+]$. Then

$$\int_{a_P^+-t+t^*}^{a_P^+} k_P(a)\nu_P(a,t^*)da \geq \int_{a_P^+-t+t^*}^{a_P^+}\int_0^{a_P^+-a} K_P(a+\sigma)\nu_P(a+\sigma,t^*+\sigma)d\sigma da$$
$$= \int_0^{t-t^*}\int_{a_P^+-\sigma}^{a_P^+} K_P(a)\nu_P(a,t-\sigma)dad\sigma.$$

Since (3.28) contradicts (3.26) we have that (3.25) is true.

We now prove that $T = +\infty$ by contradiction, assuming that $T < +\infty$. First we note that

$$\lambda_S = \sup_{t\in[0,T)} N(t) = N_{max}. \tag{3.29}$$

In fact, if $\lambda_S < N_{max}$ we can find $\lambda \in (\lambda_S, N_{max})$ so that

$$N(t) < \lambda < N_{max} \quad \text{for all} \quad t \in [0,T)$$

and consequently $t_\lambda > T$, contradicting the definition of T.

Now we consider $N(t)$ and use A2 and (3.22) to chose $N^{**} > N_P^*$ such that

$$H(N^{**})(\bar\eta_D \wedge \bar\beta_A)(N^{**} - N_P^*) > Ce^{\alpha T}.$$

Then, thanks to (3.29), we find $t^{**} < T$ and $\varepsilon < a_P^+ \wedge a_D^* \wedge a_A^+$ such that

$$N(t^{**}) = N^{**} \qquad \text{and} \qquad N(t) > N^{**} \quad \text{for} \quad t^{**} < t \leq t^{**} + \varepsilon. \tag{3.30}$$

Considering

$$N_D(t) = \int_0^{a_D^*} k_D(a)\nu_D(a,t)da \quad \text{and} \quad N_A(t) = \int_0^{a_A^+} k_A(a)\nu_A(a,t)da,$$

since (3.25) holds, we have

$$N_D(t) + N_A(t) = N(t) - N_P(t) \geq N^{**} - N_P^* > 0 \quad \text{for} \quad t \in (t^{**}, t^{**}+\varepsilon).$$

Considering all three equations (3.2), (3.3), (3.4), by similar calculations and estimates as those performed for $N_P(t)$, using (3.22), we have, for $t \in (t^+, t^+ + \varepsilon)$,

$$\begin{aligned} N(t) \leq\ & N(t^{**}) + Ce^{\alpha T}(t-t^{**}) \\ & - \int_0^{t-t^{**}}\int_\sigma^{a_D^*+\sigma} H(N(t-\sigma))\eta_D^1(a-\sigma)k_D(a-\sigma)\nu_D(a-\sigma,t-\sigma)dad\sigma \\ & - \int_0^{t-t^{**}}\int_\sigma^{a_A^+-\sigma} H(N(t-\sigma))\beta_A^1(a-\sigma)k_A(a-\sigma)\nu_A(a-\sigma,t-\sigma)dad\sigma \\ \leq\ & N^{**} + \int_0^{t-t^{**}} \left[Ce^{\alpha T} - (\bar\eta_D \wedge \bar\beta_A)H(N^{**})\left(N_P(t-\sigma) + N_A(t-\sigma)\right)\right] d\sigma \\ \leq\ & N^{**} + \left[Ce^{\alpha T} - (\bar\eta_D \wedge \bar\beta_A)H(N^{**})\left(N^{**} - N_P^*\right)\right](t-t^{**}) < \quad N^{**}. \end{aligned} \tag{3.31}$$

This last inequality contradicts (3.30). In conclusion we have $T = +\infty$ and the thesis is proved. ∎

4. Steady states. In order to consider stationary states of system (3.2)–(3.5), we suppose that the cell mortality and the mean number of viable daughter cells after a cell division do not depend on time ($\mu_P(a,t)=\mu_P(a), \mu_D(a,t)=\mu_D(a), r(t)=r$). Then a steady state will be given by a solution of the following system of time independent equations, with their respective conditions at $a=0$:

$$\begin{aligned} &\nu_P'(a)+\mu_P(a)\nu_P(a)=0,\\ &\nu_P(0)=r\theta(N)\int_0^{a_P^+} K_P(a)\nu_P(a)da, \end{aligned} \tag{4.1}$$

$$\begin{aligned} &\nu_D'(a)+(\eta_D^1(a)H(N)+\mu_D(a))\nu_D(a)=0,\\ &\nu_D(0)=r(1-\theta(N))\int_0^{a_P^+} K_P(a)\nu_P(a)da, \end{aligned} \tag{4.2}$$

$$\begin{aligned} &\nu_A'(a)+\beta_A^1(a)H(N)\nu_A(a)=0,\\ &\nu_A(0)=\int_0^{a_P^+}\mu_P(a)k_P(a)\nu_P(a)da+\int_0^{a_D^*}\mu_D(a)k_D(a)\nu_D(a)da\\ &\qquad +(2-r)\int_0^{a_P^+}K_P(a)\nu_P(a)da, \end{aligned} \tag{4.3}$$

where

$$N=\int_0^{a_P^+} k_P(a)\nu_P(a)da+\int_0^{a_D^*} k_D(a)\nu_D(a)da+\int_0^{a_A^+} k_A(a)\nu_A(a)da \tag{4.4}$$

satisfies the constraint

$$0\le N<N_{max}. \tag{4.5}$$

This system admits the trivial steady state corresponding to the extinction of the cell population. To find nontrivial states we introduce the functions

$$M_A(a,N)=e^{-H(N)\int_0^a\beta_A^1(\sigma)d\sigma},\quad E_D(a,N)=e^{-H(N)\int_0^a\eta_D^1(\sigma)d\sigma},$$

$$M_P^\mu(a)=e^{-\int_0^a\mu_P(\sigma)d\sigma},\quad M_D^\mu(a)=e^{-\int_0^a\mu_D(\sigma)d\sigma},$$

so that, for a fixed N, a solution to (4.1)–(4.3) has the form

$$\nu_P(a)=\nu_P(0)M_P^\mu(a),\ \nu_D(a)=\nu_D(0)M_D^\mu(a)E_D(a,N),\ \nu_A(a)=\nu_A(0)M_A(a,N), \tag{4.6}$$

where the values of $\nu_P(0)$, $\nu_D(0)$, and $\nu_A(0)$ are to be determined by imposing the boundary conditions and taking into account (4.4).

From the boundary condition of (4.1) we get the following equation for N:

$$r\theta(N)\int_0^{a_P^+}K_P(a)M_P^\mu(a)da=1.$$

Since $\theta(N)$ is decreasing, we have that this equation has one and only one positive solution smaller than N_{max} if and only if

$$r\theta(0)\int_0^{a_P^+}K_P(a)M_P^\mu(a)da>1,\quad r\theta(N_{max})\int_0^{a_P^+}K_P(a)M_P^\mu(a)da<1. \tag{4.7}$$

These conditions have a simple interpretation because the function

$$\mathcal{R}(N) = r\theta(N) \int_0^{a_P^+} K_P(a) M_P^\mu(a) da$$

is the basic reproduction number giving the number of new proliferating cells produced by one proliferating cell during its lifespan. This basic number is depending on the total number N of the basal cells and the conditions above mean that when N is low reproduction is enhanced, while it is inhibited when N is close to N_{max}. We note that since

$$\int_0^{a_P^+} K_P(a) M_P^\mu(a) da \le \int_0^{a_P^+} \beta_P(a) M_P(a) da = 1,$$

the second condition in (4.7) is always satisfied. Moreover, to satisfy the first of (4.7) (i.e., $\mathcal{R}(0) > 1$) we must have $r > 1$.

Provided that the first condition of (4.7) is satisfied, we can obtain the equilibrium value N^* of the total number of basal cells by satisfying $\mathcal{R}(N^*) = 1$, namely

$$\theta(N^*)\mathcal{R}(0) = 1, \quad \text{that is,} \quad N^* = \theta^{-1}\left(\frac{1}{\mathcal{R}(0)}\right). \tag{4.8}$$

Note that N^* cannot exceed the value of N at which $\theta(N)$ is equal to $1/2$, since always $\mathcal{R}(0) \le 2$.

Imposing to (4.6) the boundary conditions for $\nu_D(a)$ and $\nu_A(a)$, we easily obtain for the steady state

$$\begin{aligned} \nu_D^*(0) &= (\mathcal{R}(0) - 1)\, \nu_P^*(0), \\ \nu_A^*(0) &= \left(\mathcal{M}_P + \mathcal{M}_D(N^*)(\mathcal{R}(0) - 1) + \frac{2 - r}{r}\mathcal{R}(0)\right) \nu_P^*(0), \end{aligned} \tag{4.9}$$

where

$$\mathcal{M}_P = \int_0^{a_P^+} \mu_P(a) k_P(a) M_P^\mu(a) da, \quad \mathcal{M}_D(N^*) = \int_0^{a_D^*} \mu_D(a) k_D(a) M_D^\mu(a) E_D(a, N^*) da.$$

Finally, we determine $\nu_P^*(0)$ writing (4.4) at $N = N^*$ using the expressions (4.6), (4.9), obtaining

$$\nu_P^*(0) = k(N^*)\ N^*, \tag{4.10}$$

where

$$\begin{aligned} k(N^*) = \Bigg[&\int_0^{a_P^+} k_P(a) M_P^\mu(a) da + (\mathcal{R}(0) - 1) \int_0^{a_D^*} k_D(a) M_D^\mu(a) E_D(a, N^*) da \\ &+ \left(\mathcal{M}_P + \mathcal{M}_D(N^*)(\mathcal{R}(0) - 1) + \frac{2 - r}{r}\mathcal{R}(0)\right) \int_0^{a_A^+} k_A(a) M_A(a, N^*) da \Bigg]^{-1}. \end{aligned} \tag{4.11}$$

In conclusion we may state the following.

THEOREM 4.1. *For the system* (3.2)–(3.5)*, a unique nontrivial steady state, satisfying the constraint* (4.5)*, exists if and only if* $\mathcal{R}(0) > 1$.

Note that only the hypothesis A1 on $\theta(N)$ is required to satisfy the constraint (4.5) at the steady state solution. Assumptions (2.2), (2.3), A2 on $\eta_D(a,N)$, and $\beta_A(a,N)$ are not necessary; they were instead required to prove the fulfillment of (4.5) for any solution.

In correspondence with the steady state we have determined above, the cell flows that feed the suprabasal region are time independent and read (see (2.4) and (2.5))

$$\begin{aligned} S_P(a) &= \nu_P^*(0)\eta_P(a)k_P(a)M_P^\mu(a), \\ S_D(a) &= \nu_D^*(0)\eta_D(a,N^*)k_D(a)M_D^\mu(a)E_D(a,N^*), \\ S_A(a) &= \nu_A^*(0)\eta_A(a)k_A(a)M_A(a,N^*). \end{aligned} \tag{4.12}$$

Finally we are concerned with the question of stability of the steady states. Indeed, stability of the nontrivial steady state implies stability of the cell flows into the suprabasal zone and, in some sense, is responsible for the stability of the whole epidermis.

In order to analyze stability of the trivial state we linearize system (3.2)–(3.5) at $\nu_P(a) \equiv 0,\ \nu_D(a) \equiv 0,\ \nu_A(a) \equiv 0,\ N = 0$. Indeed, denoting $\omega_P(a,t)$, $\omega_D(a,t)$, $\omega_A(a,t)$, the deviation of the solution from such a state, we have

$$\begin{aligned} &\frac{\partial \omega_P}{\partial t} + \frac{\partial \omega_P}{\partial a} + \mu_P(a)\omega_P(a,t) = 0, \quad \omega_P(0,t) = r\int_0^{a_P^+} K_P(a)\omega_P(a,t)da, \\ &\frac{\partial \omega_D}{\partial t} + \frac{\partial \omega_D}{\partial a} + \mu_D(a))\omega_D(a,t) = 0, \quad \omega_D(0,t) = 0, \\ &\frac{\partial \omega_A}{\partial t} + \frac{\partial \omega_A}{\partial a} = 0, \quad \omega_A(0,t) = \int_0^{a_P^+} \mu_P(a)k_P(a)\omega_P(a)da \\ &\quad + \int_0^{a_D^*} \mu_D(a)k_D(a)\omega_D(a,t)da + (2-r)\int_0^{a_P^+} K_P(a)\omega_P(a,t)da. \end{aligned}$$

Then, looking for exponential solutions such as $e^{\lambda t}\phi_P(a), e^{\lambda t}\phi_D(a), e^{\lambda t}\phi_A(a)$ we have

$$\phi_P(a) = \phi_P(0)M_P^\mu(a), \quad \phi_D(a) = 0, \quad \phi_A(a) = \phi_A(0)M_A(a)E_A(a), \tag{4.13}$$

and λ satisfying the characteristic equation

$$r\int_0^{a_P^+} e^{-\lambda a}\beta_P(a)M_P(a)M_P^\mu(a)E_P(a)da = 1. \tag{4.14}$$

Now, if $\mathcal{R}(0) < 1$ the real part of all the roots of (4.14) is negative and the trivial steady state is asymptotically stable. If instead $\mathcal{R}(0) > 1$, at least one of the roots has positive real part and the state is unstable.

Concerning the nontrivial steady state, existing for $\mathcal{R}(0) > 1$, the same procedure leads to a characteristic equation which is far from being analytically tractable and we have to resort to numerical simulations to determine the stability of the state for different values of the parameter $\mathcal{R}(0)$. In fact, possible changes of stability of the nontrivial state may occur, giving rise to periodic solutions by Hopf bifurcations. Namely, by analyzing the characteristic equation, varying the parameter $\mathcal{R}(0)$, we should identify specific switching points for $\mathcal{R}(0)$ at which the nontrivial state loses its stability in favor of a periodic solution, or recovers stability together with the disappearance of periodic solution. In Figure 2 possible bifurcation graphs are generically

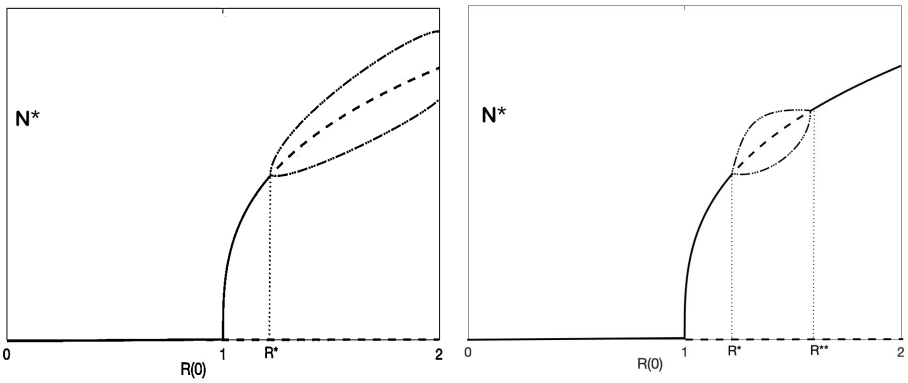

FIG. 2. *Generic bifurcation graphs showing possible scenarios for existence and stability of steady states. The total population at the steady state N^* is plotted against $\mathcal{R}(0)$. Left panel: the trivial steady state is stable (continuous line) for $\mathcal{R}(0) < 1$ and unstable (broken line) for $\mathcal{R}(0) > 1$; a nontrivial steady state arises at $\mathcal{R}(0) = 1$ inheriting the stability of the trivial one for $1 < \mathcal{R}(0) < R^*$; at $\mathcal{R}(0) = R^*$ Hopf bifurcation occurs and the steady state loses its stability, in favor of a periodic solution. Right panel: a second bifurcation of Hopf type occurs at $\mathcal{R}(0) = R^{**}$ and the nontrivial steady state recovers its stability, while the periodic solution disappears. Broken-dotted curves schematically indicate periodic solutions.*

depicted (R^* and R^{**} denote the values of $\mathcal{R}(0)$ at which Hopf bifurcation occurs), showing some classical scenarios frequently occurring in similar situations.

In the subsequent section we compute numerically solutions for various values of the parameters and analyze their behavior in order to determine stability of the nontrivial steady state. The performed simulations actually confirm that the model may present the classical bifurcation graphs shown schematically in Figure 2.

5. Numerical results. In order to make the model realistic and obtain significant numerical simulations we now choose specific functions and their parameters with an eye to experimental literature to tune the model and obtain a good approximate description of the processes occurring in the basal layer. In section 5.1 we discuss our choice of the parameters and summarize in Table 1 the baseline values used in the simulations. The numerical method we adopt to approximate the solution to (2.6)–(2.11) is based on the method of characteristics coupled with simple quadrature formulas for the integrals (see, for instance, [18]).

5.1. Parameters. We first consider proliferating cells and, for the rate of cell division $\beta_P(a)$, $0 \le a < a_P^+$, we adopt the following functional form:

$$\beta_P(a) = \hat{\beta}_P \frac{a - a_P^-}{a_P^+ - a} \, \mathbb{1}_{[a_P^-, a_P^+]}(a), \tag{5.1}$$

where $a_P^- > 0$ and a_P^+ delimit the age interval for the proliferating cells to divide (by $\mathbb{1}_I(a)$ we denote the characteristic function of the interval I). The function $\Pi_P(a) = \beta_P(a) M_P(a)$ yields the probability density function of the cell cycle time length of proliferating cells. Figure 3 (left panel) shows this density for different values of the parameter $\hat{\beta}_P$. It can be noted that the mean value of the cell cycle duration tends to a_P^+ for $\hat{\beta}_P \to 0$, whereas it tends to a_P^- for $\hat{\beta}_P$ increasing.

The mean number of viable daughter cells is assumed constant $r(t) = r = 2$, thus excluding abortive mitoses.

TABLE 1
Baseline values of model parameters.

Name	Meaning	Value	Source
a_P^-	lower bound of cell cycle time of P cells	0.8 day	[3, 30]
a_P^+	upper bound of cell cycle time of P cells	2 days	[3, 30]
a_P^*	minimal age for the detachment of P cells	0.5 days	assumed
a_D^*	upper bound of age of D cells	3 days	assumed
a_A^-	lower bound of age for the degradation of A cells	0 days	[17, 8]
a_A^+	upper bound of age of A cells	3 days	[17, 8]
$\hat{\beta}_P$	coefficient of the proliferation rate	10 day^{-1}	assumed
$\bar{\eta}_P$	detachment rate of P cells	0 day^{-1}	assumed
$\bar{\eta}_D^0$	detachment rate of D cells of age zero (for $N \to 0$)	0 day^{-1}	assumed
$\hat{\eta}_D^0$	age-dependent detachment rate of D cells coefficient	0.4 day^{-1}	assumed
$\hat{\eta}_D^1$	N-dependent detachment rate of D cells coefficient	0.01 day^{-1}	assumed
$\bar{\eta}_A$	detachment rate of A cells	0 day^{-1}	assumed
$\hat{\beta}_A^0$	age-dependent degradation rate of A cells coefficient	1 day^{-1}	assumed
$\hat{\beta}_A^1$	N-dependent degradation rate of A cells coefficient	0.02 day^{-1}	assumed
r	mean number of viable daughter cells	2	–
$\bar{\mu}_P$	rate of apoptosis of P cells	0 day^{-1}	assumed
$\bar{\mu}_D$	rate of apoptosis of D cells	0 day^{-1}	assumed
N_{max}	maximal density of basal cells	0.0138 μm^{-2}	[25, 1]
χ	shape parameter of function θ	0.95	assumed
p	shape parameter of function θ	3	assumed

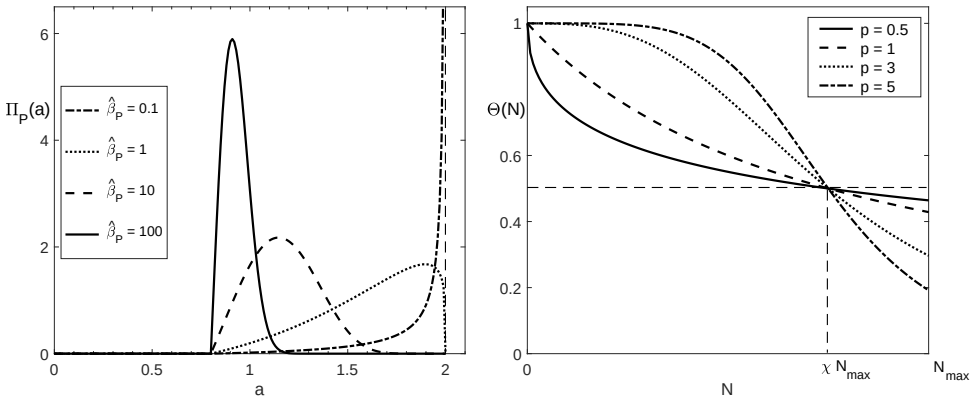

FIG. 3. *Left panel: the function* $\Pi_P(a) = \beta_P(a)M_P(a)$ *for different values of* $\hat{\beta}_P$, $a_P^- = 0.8$, $a_P^+ = 2$. *Right panel: the function* $\theta(N)$ *for* $\chi = 0.75$ *and different values of* p.

The function $\theta(N)$ regulating the fate of dividing cells is chosen of the form

$$\theta(N) = \frac{\chi^p}{\chi^p + \left(\frac{N}{N_{max}}\right)^p}. \tag{5.2}$$

This function is actually chosen for its simplicity. It, however, captures the main aspect of the phenomenon, placing at $N = \chi N_{max}$ the switching point, i.e., the value of N corresponding to a production of differentiating cells equal to that of proliferating ones. Moreover the choice of the parameter p allows us to fix how fast the differentiation occurs with cell crowding. In Figure 3 (right panel) the graph of this function is shown for different values of p.

Concerning the detachment rates, for $\eta_P(a)$, the rate at which (in a pathological situation) proliferating cells leave the basal layer, we take

$$\eta_P(a) = \bar{\eta}_P \ \mathbb{1}_{[a_P^*, a_P^+]}(a),$$

where $a_P^* \geq 0$ is the minimal age required by proliferating cells to detach from the basal layer, whereas for the rate $\eta_D(a, N)$, according to (2.2), we assume the expression

$$\eta_D(a, N) = \bar{\eta}_D^0 + \hat{\eta}_D^0 \frac{a}{a_D^* - a} + \hat{\eta}_D^1 H(N), \quad a \in [0, a_D^*), \quad N \in [0, N_{max}),$$

with

$$H(N) = \frac{N}{N_{max} - N}. \tag{5.3}$$

Moreover, we take $\eta_A(a) = \bar{\eta}_A$ constant for $0 \leq a \leq a_A^+$.

For the dissolution rate of dead cells (2.3) we assume (for $N \in [0, N_{max})$)

$$\beta_A(a, N) = \hat{\beta}_A^0 \frac{a - a_A^-}{a_A^+ - a} \ \mathbb{1}_{[a_A^-, a_A^+]}(a) + \hat{\beta}_A^1 H(N)$$

with $a_A^- \geq 0$.

Finally, the mortality rates $\mu_P(a, t)$, $\mu_D(a, t)$ are assumed constant and equal to $\bar{\mu}_P$ and $\bar{\mu}_D$, respectively. All the costants are nonnegative.

The baseline values of parameters are reported in Table 1. The values of a_P^-, a_P^+ and a_A^-, a_A^+ are chosen from the literature (see [3, 30]) to match plausible durations of the cell cycle of proliferating cells in human epidermis (the choice of $\hat{\beta}_P$ corresponds to an average duration of 1.9 days) and, respectively, of the time needed for the dissolution and reabsorption of dead cells ($\hat{\beta}_A^0$ and $\hat{\beta}_A^1$ correspond to an average time of 0.9 days). It must be stressed, however, that a remarkable uncertainty affects the knowledge of these times. Concerning the mean cell cycle duration of proliferating cells, values from 23–39 h [3, 30] to 62.5 h [5] have been estimated. Likewise, by the use of different techniques, different values of the fraction of proliferating cells (growth fraction) have been found, from 60% [13] to 20% [15]. The above baseline values and those of the parameters $\bar{\eta}_D$, $\hat{\eta}_D^0$, $\hat{\eta}_D^1$ allow us to obtain a growth fraction within the above limits.

The detachment rate $\bar{\eta}_P$ of proliferating cells is set to zero to simulate a normal, nonpathological epidermis in which cell proliferation is essentially confined to the basal layer. For the parameters χ and p of the function $\theta(N)$, the assumed values ($\chi = 0.95$ and $p = 3$) allow a surface cell density in agreement with the close-packing of basal cells [25]. It appears reasonable that cell-to-cell mechanical interactions can affect cell proliferation only over some threshold of cell crowding. This suggests a down-concavity of the function $\theta(N)$ for N small and motivates the choice of $p = 3$. Measurements of the volume of basal cells have found values in the range of 600 to 700 μm^3 [1] (see also [25]). Then the maximal surface density N_{max} was computed assuming the basal layer as formed by a monolayer of cubic cells having edge length of 8.5 μm (and cell volume of 614.125 μm^3), so obtaining the value of 0.0138 cells$\cdot\mu$m^{-2}.

Finally, we will take $\bar{\eta}_A = 0$ in all simulations, so excluding the hypothetical pathological occurrence of a transfer of apoptotic cells into the suprabasal zone.

5.2. The stationary state of the normal epidermis. We start by computing the stationary state of the system, described in section 4, with the baseline parameter values of Table 1. These correspond to the case of *noninjured* ($\bar{\mu}_P = \bar{\mu}_D = 0$) and *nonpathological* ($\bar{\eta}_P = 0$) epidermis. The cell population age densities at the stationary state are shown in Figure 4 (left panel). Since detachment and death of proliferating cells are null, R_0 is equal to 2 and so $N^*/N_{max} = \chi$, i.e., this ratio is equal to 0.95. The fractions of proliferating cells and differentiated cells in the basal population are equal to 41.1% and 58.9%, respectively.

We studied the stability of this equilibrium by computing numerically the time-evolution of system (2.6)–(2.9) from different initial conditions. These simulations suggest that the stationary state is (asymptotically) stable, and Figure 4 (right panel) shows an example of the convergence of $N(t)$ to the equilibrium value N^*. Moreover, the term $\hat{\eta}_D^1 H(N)$ in the detachment rate of differentiated cells appears to have a stabilizing effect. In fact (see Figure 5), persistent oscillations of $N(t)$ arise decreasing $\hat{\eta}_D^1$ from the baseline value of Figure 4 ($\hat{\eta}_D^1 = 10^{-2}$). However, note that $N(t)$ never overcomes N_{max} as long as $\hat{\eta}_D^1 > 0$, according to Theorem 3.3. Instead, N_{max} is crossed for $\hat{\eta}_D^1 = 0$ (see Figure 5).

5.3. The injured epidermis. Next, we consider the case in which the normal epidermis is under the action of an injuring agent (e.g., UV rays) that induce cell death. Assuming $\bar{\mu}_P = \bar{\mu}_D = 0.08$ day^{-1}, the fraction of apoptotic cells at the stationary state is equal to 9.8% (proliferating cells 39.7%, differentiated cells 50.5%). The cell population age densities at the stationary state are reported in Figure 6 (left panel). Due to the presence of cell death, $\mathcal{R}(0)$ is smaller than 2 and is equal to 1.821. So the ratio N^*/N_{max} reduces to 0.89 as predicted by (4.9). This new steady state appears to be stable (see Figure 6, right panel).

Comparing the right panel of Figure 6 with the right panel of Figure 4, we can observe that in the presence of mortality the convergence of $N(t)$ to the stationary value is less damped. Thus, injury has a destabilizing effect on the steady state and challenges the basal layer homeostasis. Indeed, it can be of interest to investigate numerically how stability changes with the two parameters $\hat{\eta}_D^1$ and $\mu = \bar{\mu}_P = \bar{\mu}_D$. Figure 7 shows the stability regions in the plane $(\mu, \hat{\eta}_D^1)$ for different values of $\hat{\beta}_A^1$

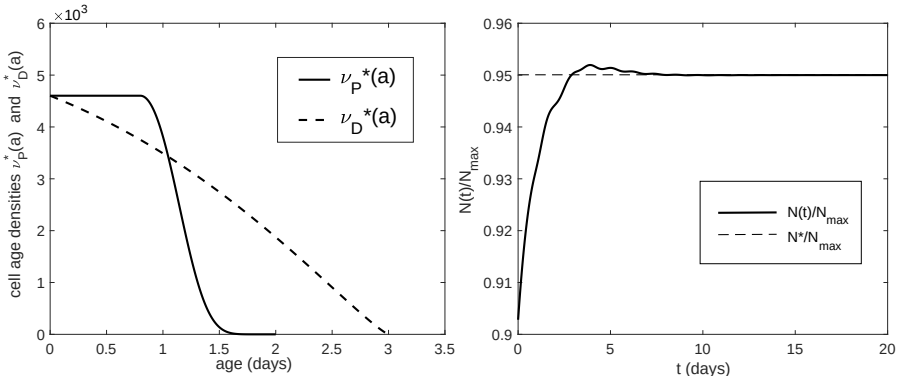

FIG. 4. *The normal epidermis (parameters as in Table* 1*). Left panel: cell age densities at the steady state (*cells $\times$ mm^{-2} $\times$ day^{-1}*); proliferating cells account for* 41.1*% of the basal population and differentiated cells for the remaining* 58.9*%. Right panel: evolution of* $N(t)$ *starting from the initial condition* $\nu_P^0(a) = 0.95\,\nu_P^*(a)$, $\nu_D^0(a) = 0.95\,\nu_D^*(a)$.

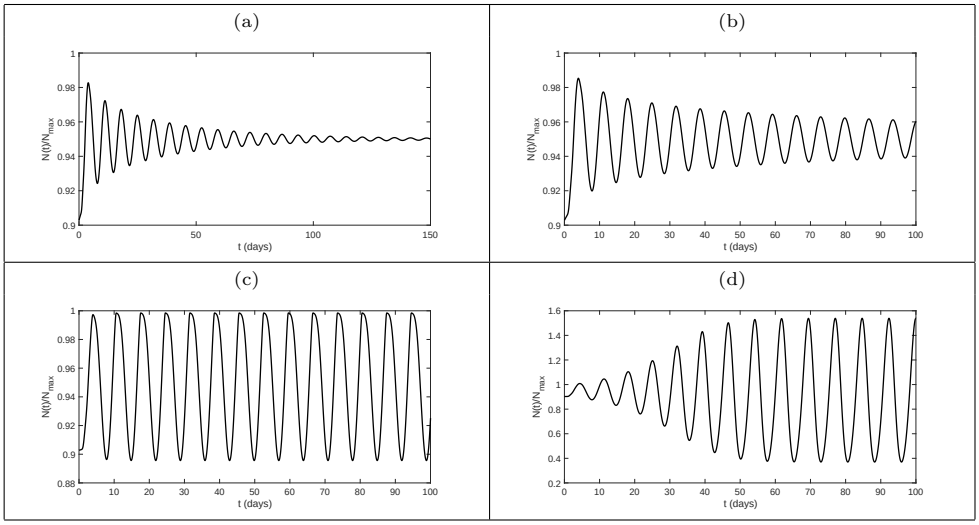

FIG. 5. *The effect of the term* $\hat{\eta}_D^1 H(N)$ *on stability.* (a) $\hat{\eta}_D^1 = 10^{-3}$, *the steady state is asymptotically stable and the solution oscillate;* (b) $\hat{\eta}_D^1 = 0.78 \times 10^{-3}$, $N(t)$ *tends to a periodic solution with small amplitude, and this case can be considered the switching point from stability to instability;* (c) $\hat{\eta}_D^1 = 10^{-4}$, *the solution is unstable;* (d) $\hat{\eta}_D^1 = 0$, *the solution is unstable and overcomes* N_{max}.

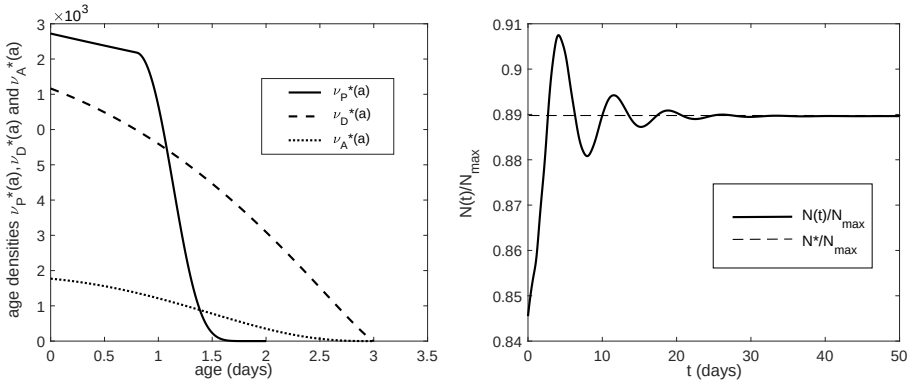

FIG. 6. *The injured epidermis. Left panel: cell age densities at the steady state (*cells $\times$ mm$^{-2} \times$ day^{-1}*); here* $\bar{\mu}_P = \bar{\mu}_D = 0.08$ *day*$^{-1}$ *(*$R_0 = 1.821$*), other parameters as in Table* 1. *The fraction of apoptotic cells at the stationary state is equal to* 9.8% *(proliferating cells* 39.7%*, differentiated cells* 50.5%*). Right panel: evolution of* $N(t)$ *starting from the initial condition* $\nu_P^0(a) = 0.95\,\nu_P^*(a)$, $\nu_D^0(a) = 0.95\,\nu_D^*(a)$, $\nu_A^0(a) = 0.95\,\nu_A^*(a)$.

(note that in the limit $\hat{\beta}_A^1 \to \infty$ the dissolution is instantaneous if $a_A^- = 0$, and then the percentage of dead cells in the basal layer is zero even if cell death occurs). For each curve the stable region is the one over the curve.

Based on the results shown in Figure 7 and noticing that $\mathcal{R}(0)$ is decreasing with μ, we can reproduce the scenarios conjectured in Figure 2. In fact, taking, for instance, $\hat{\eta}_D^1 = 0.5$, we have the scenario illustrated in the left panel of Figure 2, while for $\hat{\beta}_A^1 = \infty$ and taking $\hat{\eta}_D^1 = 1.3$ we have the case of the right panel.

5.4. The pathological epidermis. Finally, we have studied the steady state of a pathological epidermis in which the migration of proliferating cells from the basal

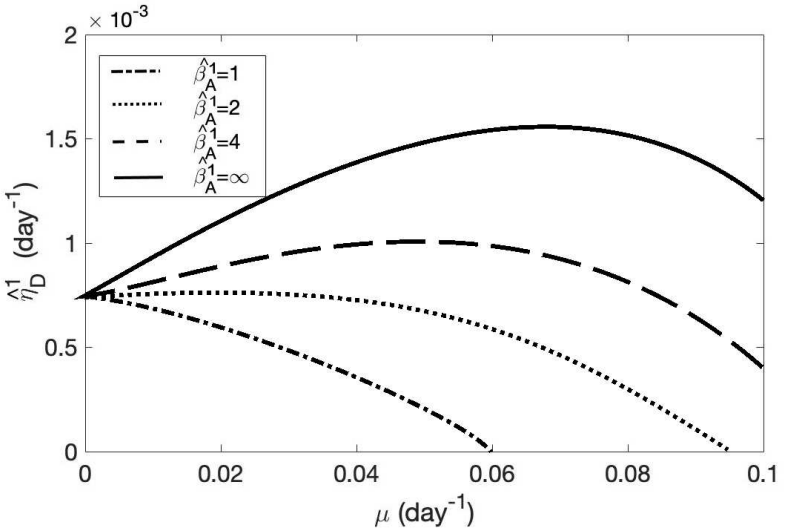

FIG. 7. *Stability regions in the plane* $(\mu, \hat{\eta}_D^1)$ *for different values of* $\hat{\beta}_A^1$. *Stability occurs for parameters over the curve. Other parameters as in Table* 1.

layer cannot be disregarded. The detachment rate $\bar{\eta}_P$ was varied from zero to 1 day^{-1} in the absence of cell death, and the numbers of proliferating and differentiated cells that move to the suprabasal region per unit time and per unit surface have been computed at the steady state by integrating with respect to age the quantities $S_P(a)$ and $S_D(a)$ given in (4.12). Indeed we have

$$J_P^* = \int_0^{a_P^+} S_P(a)da = \nu_P^*(0)\bar{\eta}_P \int_{a_P^*}^{a_P^+} M_P(a)E_P(a)da,$$
$$J_D^* = \int_0^{a_D^*} S_D(a)da = \nu_D^*(0). \tag{5.4}$$

Figure 8 (left panel) reports the graphs of these quantities as functions of $\bar{\eta}_P$ in the two cases $a_P^* = 0.5$ and $a_P^* = 0.8$ day. As expected, since only the proliferating cells with age larger than a_P^* are allowed to leave the basal layer, their flow is reduced when a_P^* increases. Moreover, one can note the continuous decrease of the flow of differentiated cells as $\bar{\eta}_P$ increases, whereas the expected increase of the proliferating cell flow is not maintained at high values of the detachment rate where instead a decline can be observed. This fact is explained by the behavior of the density of proliferating cells (see the right panel of Figure 8, where the case of $a_P^* = 0.5$ day is shown): as $\bar{\eta}_P$ increases, this density first keeps on a plateau and eventually drops. The right panel of Figure 8 also shows a decline of the total basal-layer cell density; indeed the ratio N^*/N_{max} decreases from 0.95 to 0.32, namely to a value indicating the complete loss of the close-packing condition. The substantial constancy of the proliferating cell density up to $\bar{\eta}_P = 0.8$ day^{-1} can be surprising since the proliferating cell outflow is increasing. However, it must be noted that when the total density N is decreasing, the balance between the production of proliferating cells and of differentiated cells is displaced in favor of proliferating cells, since the fraction θ increases as N decreases. This mechanism, which appears to guarantee some homeostasis of the proliferating cell density, eventually fails because the function $\theta(N)$, with the chosen value of p, is saturating as N goes to zero.

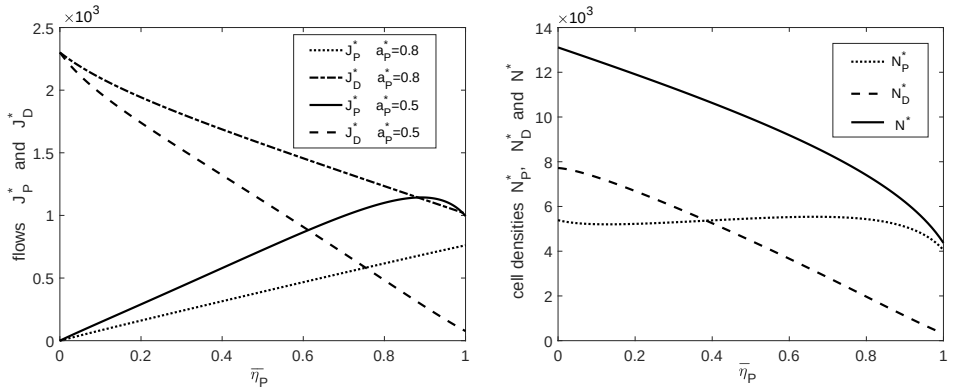

FIG. 8. *The pathological epidermis. Left panel: cell flows* J_P^* *and* J_D^* *(*cells $\times$ mm^{-2} $\times$ day^{-1}*) leaving the basal layer at the steady state for different values of* $\bar{\eta}_P$ *(day*$^{-1}$*), in the case* $a_P^* = 0.5$ *or* $a_P^* = 0.8$ *day as indicated. Other parameters as in Table* 1*. Right panel: cell densities* N_P^**,* N_D^**, and* N^* *(*cells $\times$ mm^{-2}*) at the steady state for different values of* $\bar{\eta}_P$ *(day*$^{-1}$*) in the case* $a_P^* = 0.5$ *day.*

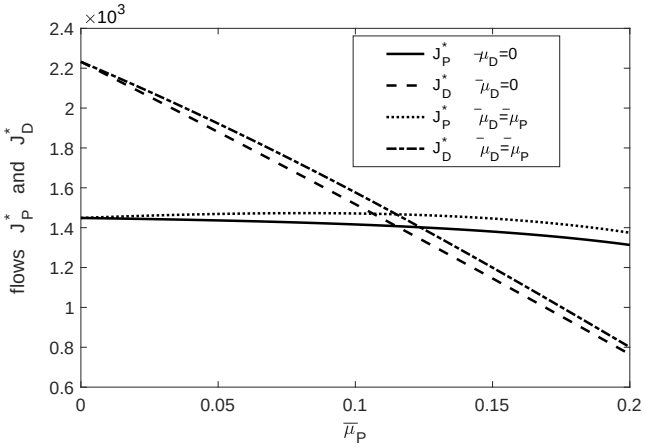

FIG. 9. *The pathological epidermis: cell flows (*cells $\times$ mm^{-2} $\times$ day^{-1}*) leaving the basal layer at the steady state for different values of* $\bar{\mu}_P$ *(day*$^{-1}$*) and* $\bar{\eta}_P = 0.5$ *(day*$^{-1}$*). The two cases* $\bar{\mu}_D = 0$ *or* $\bar{\mu}_D = \bar{\mu}_P$ *are indicated. Other parameters as in Table* 1*.*

In a pathological condition of hyperproliferation, i.e., when cell proliferation expands into the suprabasal region, the use of cell killing agents could be suggested as a treatment. To explore the effects of this therapeutic approach on the basal layer, we simulated the cell flows in the presence of cell death. Figure 9 shows the flows of proliferating and differentiated cells toward the suprabasal region as a function of $\bar{\mu}_P$ for $\bar{\eta}_P = 0.5$ and when the differentiated cells have two different sensitivities to therapy: $\bar{\mu}_D = 0$ and $\bar{\mu}_D = \bar{\mu}_P$. The stable flow of proliferating cells when $\bar{\mu}_P$ increases reveals that the density of proliferating cells is maintained almost constant, as in the case of Figure 8 (right panel), confirming the homeostatic role of the feedback $\theta(N)$. When also differentiated cells are killed, unexpectedly, both flows are increased. This fact can be explained taking into account that for a given value of $\bar{\mu}_P$, the value of N^* is the same for the two patterns of $\bar{\mu}_D$, whereas, according to (4.11), $k(N^*)$

increases when $\bar{\mu}_D \neq 0$. Thus $\nu_P^*(0)$ and $\nu_D^*(0)$ increase (see (4.10) and (4.9)), as well as the flows (see (5.4)). The above results bring into question the advantages of targeting the basal proliferating cells, since the system appears capable of sparing this cell compartment at the expense of the compartment of the differentiated cells.

6. Conclusions. The model presented in the previous sections tries to set up a realistic scenario for the dynamics of cell production and growth within the basal layer of the epidermis. It includes nonlinear feedback mechanisms, controlling proliferation, detachment, and dissolution, to guarantee the fulfillment of the physical constraint on the surface cell density, imposed by the cell occupancy of the basement membrane.

First, well-posedness of the model was proved, under general conditions, by iterative procedures allowed by suitable estimates. Then, by specific assumptions on the rates the model has been explored to investigate the effect of key parameters.

By numerical simulations in which the values of some basic parameters have been taken from the literature, we have investigated the conditions under which stability occurs both in the normal case of a noninjured, healthy epidermis and in some pathological situations. The results show that the interplay of the mechanism of cell production with the mechanism of detachment produces a substantial homeostasis of the compartment of proliferating cells. This homeostasis, however, can be ultimately perturbed up to destabilization.

The analysis of the dynamics within the basal layer, other than per se, is interesting in view of a complete model of epidermis, including the dynamics occurring in the suprabasal region. In fact, in the context proposed in [10, 11, 12], the present model provides an input to the suprabasal layers through the fluxes given in (2.4)–(2.5) or, in the case of a steady state, in (4.12).

We want to stress that the model we have proposed is somewhat basic and simple, since it does not take into account many aspects of the typical complexity of biological tissues. It is, however, a first step, open to implementation and asking for further work. The most important development should be the introduction of spatial structure devising mechanisms for cells movement that would allow modeling pathologies such as tumor developments. In such a case, the control feedback defined by assumption A1 is likely to be inactive since the mechanism of cell-cell contact inhibition is dysregulated in tumor cells. Then, we can expect $\theta(N_{max}) > 1/2$. Moreover, the spatial structure would be fundamental because lateral motion of cells cannot be disregarded. In case of basaliomas, as well as other epidermal tumors, the cell motion should be fully described, in both the lateral and orthogonal components.

REFERENCES

[1] P. R. Bergstresser, R. J. Pariser, and J. R. Taylor, *Counting and sizing of epidermal cells in normal human skin*, J. Invest. Dermatol., 70 (1978), pp. 280–284

[2] F. Bernerd, A. Sarasin, and T. Magnaldo, *Galectin-7 overexpression is associated with the apoptotic process in UVB-induced sunburn keratinocytes*, Proc. Natl. Acad. Sci. USA., 96 (1999), pp. 11329–11334

[3] J. B. Boezeman, F. W. Bauer, and R. M. de Grood, *Flow cytometric analysis of the recruitment of G0 cells in human epidermis in vivo following tape stripping*, Cell Tissue Kinet., 20 (1987), pp. 99–107

[4] A. Bordbar, D. Dias, A. Cabral, S. Beck, and M. E. Boon, *Assessment of cell proliferation in benign, premalignant and malignant skin lesions*, Appl. Immunohistochem. Mol. Morphol., 15 (2007), pp. 229–235.

[5] F. A. Castelijns, J. Ezendam, M. A. Latijnhouwers, I. M. Van Vlijmen-Willems, P. L. Zeeuwin, M. J. Gerritsen, P. C. Van de Kerkhof, and P. E. Van Erp, *Epidermal cell kinetics by combining in situ hybridization and immunohistochemistry*, Histochem. J., 30 (1998), pp. 869–877

[6] M. A. Chaplain, L. Graziano, and L. Preziosi, *Mathematical modelling of the loss of tissue compression responsiveness and its role in solid tumour development*, Math. Med. Biol., 23 (2006), pp. 197–229.
[7] E. Clayton, D. P. Doupe, A. M. Klein, D. J. Winton, B. D. Simons, and P. H. Jones, *A single type of progenitor cell maintains normal epidermis*, Nature, 446 (2007), pp. 185–189.
[8] Z. Darzynkiewicz, G. Juan, X. Li, W. Gorczyca, T. Murakami, and F. Traganos, *Cytometry in cell necrobiology: Analysis of apoptosis and accidental cell death (necrosis)*, Cytometry, 27 (1997), pp. –20.
[9] A. d'Onofrio and I. P. M. Tomlinson, *A nonlinear mathematical model of cell turnover, differentiation and tumorigenesis in the intestinal crypt*, J. Theoret. Biol., 244 (2007), pp. 367–374.
[10] A. Gandolfi, M. Iannelli, and G. Marinoschi, *An age-structured model of epidermis growth*, J. Math. Biol., 62 (2011), pp. 111–141.
[11] A. Gandolfi, M. Iannelli, and G. Marinoschi, *Time evolution for a model of epidermis growth*, J. Evol. Equ., 13 (2013), pp. 509–533.
[12] A. Gandolfi, M. Iannelli, and G. Marinoschi, *The steady state of epidermis: Mathematical modeling and numerical simulations*, J. Math. Biol., 73 (2016), pp. 1595–1626.
[13] S. Gelfant, *On the existence of non-cycling germinative cells in human epidermis in vivo and cell cycle aspects of psoriasis*, Cell Tissue Kinet., 15 (1982), pp. 393–397.
[14] S. Ghazizadeh and L. B. Taichman, *Organization of stem cells and their progeny in human epidermis*, J. Invest. Dermatol., 124 (2005), pp. 367–372.
[15] M. Heenen, S. Thiriar, J. C. Noël, and P. Galand, *Ki*-67 *immunostaining of normal human epidermis: Comparison with* 3*H-thymidine labelling and PCNA immunostaining*, Dermatology, 197 (1998), pp. 123–126.
[16] E. Houben, K. De Paepe, and V. Rogiers, *A keratinocyte's course of life*, Skin Pharmacol. Physiol., 20 (2007), pp. 122–32.
[17] Z. Hu, K. Yuri, H. Ozawa, H. Lu, and M. Kawata, *The in vivo time course for elimination of adrenalectomy-induced apoptotic profiles from the granule cell layer of the rat hippocampus*, J. Neurosci., 17 (1997), pp. 3981–3989.
[18] M. Iannelli and F. A. Milner, *The Basic Approach to Age-Structured Population Dynamics: Models, Methods and Numerics*, Lect. Notes Math. Model. Life Sci., Springer, New York, 2017.
[19] S. Ipponjima, T. Hibi, and T. Nemoto, *Three-dimensional analysis of cell division orientation in epidermal basal layer using intravital two-photon microscopy*, PLoS One, 11 (2016), e0163199.
[20] K. B. Jensen and F. M. Watt, *Single-cell expression profiling of human epidermal stem and transit-amplifying cells: Lrig*1 *is a regulator of stem cell quiescence*, Proc. Natl. Acad. Sci. USA, 103 (2006), pp. 11958–11963.
[21] M. D. Johnston, C. M. Edwards, W. F. Bodmer, P. K. Maini, and S. J. Chapman, *Mathematical modeling of cell population dynamics in the colonic crypt and in colorectal cancer*, Proc. Natl. Acad. Sci. USA, 104 (2007), pp. 4008–4013.
[22] P. H. Jones, B. D. Simons, and F. M. Watt, *Sic transit gloria: farewell to the epidermal transit amplifying cell?*, Cell Stem Cell, 1 (2007), pp. 371–381.
[23] P. Kaur and C. S. Potten, *The interfollicular epidermal stem cell saga: Sensationalism versus reality check*, Experim. Dermatol., 20 (2011), pp. 697–702.
[24] K. Kawashima, H. Doi, Y. Ito, M. A. Shibata, R. Yoshinaka, and Y. Otsuki, *Evaluation of cell death and proliferation in psoriatic epidermis*, J. Dermatol. Sci., 35 (2004), pp. 207–214.
[25] A. J. P. Klein-Szanto, *Clear and dark basal keratinocytes in human epidermis. A stereologic study*, J. Cutan. Pathol., 4 (1977), pp. 275–280.
[26] T. Lechler and E. Fuchs, *Asymmetric cell divisions promote stratification and differentiation of mammalian skin*, Nature, 437 (2005), pp. 275–280.
[27] X. Lim, S. H. Tan, W. L. C. Koh, R. M. W. Chau, K. S. Yan, C. J. Kuo, R. van Amerongen, A. M. Klein, and R. Nusse, *Interfollicular epidermal stem cells self-renew via autocrine Wnt signaling*, Science, 342 (2013), pp. 1226–1230.
[28] G. Mascré, S. Dekoninck, B. Drogat, K. K Youssef, S. Brohée, P. A. Sotiropoulou, B. D. Simons, and C. Blanpain, *Distinct contribution of stem and progenitor cells to epidermal maintenance*, Nature, 489 (2012), pp. 257–262.
[29] N. D. Poulson and T. Lechler, *Asymmetric cell divisions in the epidermis*, Int. Rev. Cell Mol. Biol., 295 (2012), pp. 199–232.
[30] J. J. Rijzewijk, J. B. Boezeman, and F. W. Bauer, *Synchronized growth in human epidermis following tape-stripping: Its implication for cell kinetic studies*, Cell Tissue Kinet., 21 (1988), pp. 227–129.

[31] P. Rompolas, K. R. Mesa, K. Kawaguchi, S. Park, D. Gonzalez, S. Brown, J. Boucher, A. M. Klein, and V. Greco, *Spatiotemporal coordination of stem cell commitment during epidermal homeostasis*, Science, 352 (2016), pp. 1471–1474.
[32] A. Sada, F. Jacob, E. Leung, S. Wang, B. S. White, D. Shalloway, and T. Tumbar, *Defining the cellular lineage hierarchy in the interfollicular epidermis of adult skin*, Nature Cell Biol., 18 (2016), pp. 619–631.
[33] N. J. Savill, *Mathematical models of hierarchically structured cell populations under equilibrium with application to the epidermis*, Cell Prolif., 36 (2003), pp. 1–26.
[34] F. M. Watt, *Stem cell fate and patterning in mammalian epidermis*, Curr. Opin. Genet. Develop., 11 (2001), pp. 410–417.
[35] H. Zhang, W. Hou, L. Henrot, S. Schnebert, M. Dumas, C. Heuséle, and J. Yang, *Modelling epidermis homoeostasis and psoriasis pathogenesis*, J. R. Soc. Interface, 12 (2015), 20141071.